An Auditory Model with Hearing Loss

Nielsen, Lars Bramsløw

Publication date:
1993

Document Version
Publisher's PDF, also known as Version of record

ISSN 0105-3027

An Auditory Model with Hearing Loss

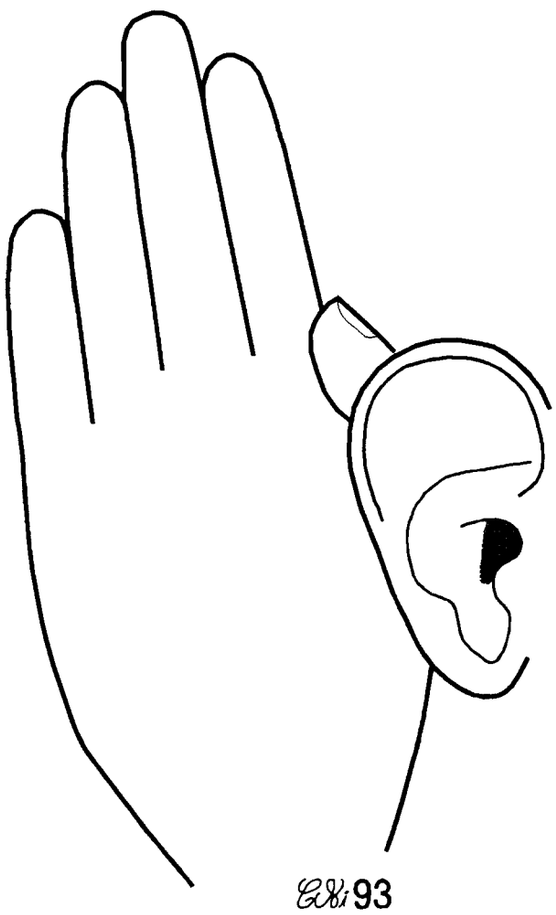

THE ACOUSTICS LABORATORY

TECHNICAL UNIVERSITY OF DENMARK

Report No. 52, 1993

An Auditory Model with Hearing Loss.

by

Lars Bramsløw Nielsen

Oticon Research Unit "Eriksholm"

and

The Acoustics Laboratory
Technical University of Denmark

Abstract.

An auditory model based on the psychophysics of hearing has been developed and tested. The model simulates the normal ear or an impaired ear with a given hearing loss. Based on reviews of the current literature, the frequency selectivity and loudness growth as functions of threshold and stimulus level have been found and implemented in the model.

The auditory model was verified against selected results from the literature, and it was confirmed that the normal spread of masking and loudness growth could be simulated in the model. The effects of hearing loss on these parameters was also in qualitative agreement with recent findings. The temporal properties of the ear have currently not been included in the model.

As an example of a real-world application of the model, loudness spectrograms for a speech utterance were presented. By introducing hearing loss, the speech sounds became less audible and less detailed, a problem that linear amplification did not solve properly. This demonstrated how the model could be used for hearing aid development and evaluation.

Preface.

This report describes the development and structure of an auditory model for objective evaluation of sound quality in hearing aids. Since the model is intended to model a hearing-impaired listener, the hearing loss has been included as a parameter in the model, affecting sensitivity as well as frequency resolution and loudness perception. Such a model should attempt to unite all known aspects of psychoacoustics for normal-hearing and hearing-impaired listeners into a coherent picture, which is obviously an impossible goal. The current model is a result of many compromises and represents a first, simplistic attempt at such a unification.

The report deals with many psychoacoustic terms in a limited amount, and is thus on a fairly advanced level. The reader is expected to be familiar with basic psychoacoustics, to read the report with a good understanding. Good introductory texts can be found in Zwicker & Fastl (1990), Scharf & Buus (1986) and Scharf & Houtsma (1986).

The model is just one of the elements covered in the entire Ph.D. project "Modeling of sound quality for hearing-impaired listeners", and limited time has thus been available for exploration of a large and complex topic. The Ph.D. project is a joint project between Oticon A/S and The Acoustics Laboratory, Technical University of Denmark, and the report has thus been published by both parties: Oticon Internal Report No. 43-8-2 and The Acoustics Laboratory, Technical report no. 52.

I want to acknowledge my advisors for their support and valuable discussion during the work with this model: Claus Elberling, Oticon A/S, Torben Poulsen, The Acoustics Laboratory and Paul Dalsgaard, Center for Speech Technology, Aalborg University Center. Furthermore, I want to express my gratitude to Søren Buus and Mary Florentine, Northeastern University, Boston, for many critical and useful suggestions during the last phase of evaluations and modifications of the model.

Lars Bramsløw Nielsen

Snekkersten, February 1993

Table of contents.

1 Introduction.

The human auditory system is a very sophisticated and complicated signal processing system that is capable of perceiving and analyzing very complex sounds and discriminating subtle changes in sound. These characteristics are crucial for the perception and recognition of speech and for interpretation of the sound patterns encountered in daily life, as well as for enjoyment of music. The normal hearing system can be damaged due to aging, otologic diseases, exposure to loud noises, ototoxic drugs and other reasons. This will often result in a communication handicap, due to loss of sensitivity and impaired discrimination of speech sounds as well as other auditory stimuli.

Much research has been done to further our understanding of the human hearing system, but there is still very limited knowledge concerning the function of the system on a physiological level as well as on a psychological level, i.e. in the disciplines auditory physiology and psychoacoustics. Research results are often summarized in mathematical or verbal models, to explain a certain phenomenon in a meaningful way and to allow the application of the model to other similar problems. Models of psychoacoustic phenomena, such as frequency masking, have provided much insight into the function of the hearing system (Zwicker & Fastl, 1990).

When modeling functional parts of the hearing system and applying these models to for instance speech sounds, we often refer to them as cochlear models or auditory models. In the literature, these terms are sometimes used interchangeably. In this report, the term cochlear model refers to a model that takes its origin in the physiological macro- and micro-mechanics and neural function of the cochlea. An auditory model describes the auditory function on a higher "black-box" level and attempts to model psychoacoustical phenomena correctly, with little or no attention concerning a possible anatomic location, e.g. whether the characteristics are peripheral (frequency selectivity, active tuning) or more central (probably aspects of loudness and temporal resolution). Some of the auditory models in the literature are mixed, including results from both physiology and psychoacoustics.

An introduction to two of the published cochlear models and two auditory models has been given by Fink (1989), these are summarized in section 2 of the present report. None of these models include the case of impaired hearing, i.e. hearing loss. The present report describes the development and evaluation of such a model:

In section 2, literature review, a number of existing models are presented. The issues concerning cochlear (physiological) versus auditory (psychoacoustical) models are discussed. After reviewing literature on auditory models and psychoacoustical measurements, the choice of an auditory model is justified.

Section 3 is a detailed description of the model and the underlying theories and psychoacoustical test paradigms. The elements in the model are discussed: Frequency selectivity, temporal resolution, loudness coding and hearing loss. Suitable tests for verification of the model are also discussed.

In section 4 verification results for the model are presented. The purpose is to duplicate known psychoacoustic test results from the literature, by means of the model and thereby justifying that the model simulates average cases of normal and impaired hearing.

In section 5 one application of the model is demonstrated: Analysis of normal and amplified (frequency shaped) speech signals for the normal-hearing case and for a typical sensorineural, sloping hearing loss.

2 Literature review.

2.1 Cochlear models.

Several authors have presented models in the literature intended to mimic the physiological function of the cochlea more or less. One motivation for this work was to develop perceptually relevant pre-processors for automatic speech recognition systems. Partly because of this, there has been little or no interest in models of the impaired cochlea. More recently two authors have included hearing loss in their cochlear models (Allen, 1990; Kates, 1991). Understanding the functionality of cochlear models requires basic knowledge of the human auditory physiology, see for instance Pickles (1982).

Allen (1985) offers a good overview of cochlear modeling, including a summary of his own work. Models are described for the outer ear (pinnae), middle ear and cochlea, with an emphasis on the latter part. The mechanisms for the basilar membrane, Corti's organ, and tectorial membrane are discussed. A fundamental problem in cochlear micromechanics is the discrepancy between the basilar membrane mechanical tuning curves and the much sharper neural tuning curves. Two explanations are offered for this very sharp tuning exhibited by the normal cochlea. The first explanation assumes that the tectorial membrane is resonant and tuned to a slightly different frequency, thereby introducing additional zeros in the transfer function between basilar membrane motion and hair cells. The second explanation (Neely and Kim, 1983) calls upon the concept of negative damping in the basilar membrane, based on an active feedback system, in which the outer hair cells are innervated by efferent nerve fibers and act as motor cells. There is no clear evidence as to which explanation is more correct.

The output from the mechanical model is then fed to a hair-cell model, followed by zero-crossing detector. By processing speech sounds through the model, the output of this detector is used to form a "neurogram", i.e. a neural equivalent of a spectrogram, which is an x-y-z time-frequency plot of a signal. This neurogram shows some ability to enhance speech or pure tones in noise, as the human hearing system is capable of (typical detection threshold of a pure tone in narrow-band noise is at negative signal-to-noise

ratio). In a later paper (Allen, 1990), a model for the noise-damaged cochlea is described. The reduced frequency selectivity can be accounted for by a reduced stiffness of the basilar membrane. Allen offers the following hypothesis: In the normal cochlea, the BM stiffness is increased due to the active-feedback process from the outer haircells, that act as motor cells, rather than sensory cells. There is evidence that the outer haircells are damaged by noise exposure, thus reducing or destroying the active system.

The model described by Seneff (1984, 1985) contains a 40-channel critical-band filterbank, implemented as a cascade of zeroes (notch filters), followed by a resonator between each cascade section, to form a 40-channel parallel output. This filter structure simulates the basilar membrane and the traveling-wave motion along it, and sufficiently sharp tuning curves are obtained. There is no active feedback process in the filter structure. Each resonator output is then followed by two automatic gain Controls (AGC) in order to effect amplitude compression and adaptation phenomena. The signal is then fed to a saturating half-wave rectifier, acting as a hair-cell model. The outputs of this "peripheral" model is subsequently processed by a hypothesized "central" processor - an envelope/synchrony detector. This detector serves to detect prominent periodicities in the input waveform, in order to estimate fundamental frequency and formant structure for an incoming speech signal.

Lyon (1982) and Lyon & Dyer (1986) have developed a cochlear model consisting of simple second-order notch filter sections in cascade. Resonance sections mimic the tectorial membrane resonance, followed by detectors and a multi-channel AGC coupled across channels (implementing a "spatial spread" function along the basilar membrane). The model is characterized by a large number of simple processing elements and a high degree of parallelism. An analog Very Large Scale Integrated (VLSI) chip implementation is thus feasible and has been presented by Lyon and Mead (1988), with a resolution of 480 channels.

Kates (1991) has developed a digital cochlear model, that allows for a degradation related to hearing impairment. The model consists of the middle ear, the mechanical motion of the basilar membrane and the neural transduction of the hair cells. The

traveling waves on the cochlear partition are represented by a cascade of second-order resonant lowpass filters. The displacement output is then differentiated to obtain the velocity and fed through a second filter, that is hypothesized to result from the resonance in the motion between the basilar membrane and the tectorial membrane. The second filter is followed by a hair cell model, and each hair cell has four nerve fibers attached to it, using both low- and high-spontaneous firing rate fibers. In Kates' cochlear model, there is an active feedback path, that sharpens the filter selectivity at low signal levels, suggested as a simulation of an active outer hair cell feedback mechanism. Hearing impairment can be simulated by either removing the feedback (corresponding to complete loss of outer hair cells) or by removing parts of the inner hair cells hairs (stereocilia). With loss of outer hair cells, the filter system becomes linear with loss of the normally improved frequency selectivity at low levels. With loss of inner hair cell stereocilia, the overall sensitivity is reduced. This can be alleviated by amplification, however the higher signal levels will then cause a broadening of the cochlear filters.

In my opinion, Kates' model is an important step towards using cochlear models for the study of hearing impairment and potentially useful signal processing strategies, at least on a qualitative level. It is not clear, however, how a given hearing loss (expressed by the hearing thresholds in the audiogram) is simulated quantitatively. Specification of the loss of outer and inner hair cells in the model due to hearing impairment is very difficult, only rough estimates can be used. Another problem with this model as with other cochlear models, is that they are computationally very intensive. Kates' model requires 1.5 s *per* sample on an 8 MHz IBM PC-AT, which at 40 kHz sample rate means 60.000 times real time.

2.2 Physiological measurements.

All the physiologically based (cochlear) models must be based on some type of physiological measurements on humans or animals with similar auditory physiology (such as the cat). In particular, we are interested in the frequency analyzer capabilities of the cochlea, i.e. the frequency selectivity in the system. Making these physiological measurements is very difficult, since the introduction of measurement probes or other

objects in the very delicate system normally damages or at least interferes with the normal cochlear function. Therefore, there are still many unanswered questions concerning the mechanics and physiology of the cochlea. Measurements of the basilar membrane movements and mechanical tuning have been done using mechanical or optical techniques, requiring the intrusion into the cochlea for the placement of measurement probes, mirrors or other objects onto the basilar membrane. This must be done on live animals (*in vivo*), but the intrusion nevertheless ruptures membranes, disturbs the cochlear fluids and thus the cochlear potentials etc., making valid results difficult to obtain.

Another way of characterizing cochlear frequency selectivity is by means of neurophysiological measurements. This is typically done by inserting very thin measurement electrodes into single nerve fibers in the auditory nerve (8th nerve) that connects the cochlea to the brainstem. The individual fibers in the nerve are tonotopically arranged, i.e. a given fiber represents a given location along the basilar membrane. The corresponding frequency is called the Characteristic Frequency (CF) of the fiber. The frequency selectivity of a fiber, can be measured by adjusting the level of a swept pure tone up and down to maintain a constant spike activity in the nerve. The resulting curve is loosely referred to as "tuning curves", or more precisely, as Frequency Threshold Curves (FTC). Since the FTC includes the mechanical tuning system as well as hair-cell transduction and possible interaction between different regions in the cochlea, it is likely that the micro-mechanics of the cochlea cannot be deduced from the neural tuning data.

For further information on cochlear physiology and overview of measurement techniques, see for example Pickles (1982).

The shape of FTCs recorded from single nerve fibers in the 8th nerve of a cat, using a single pure tone, have been quantified by Evans (1975a). These curves show the dB SPL of a swept sine wave required to produce a constant spike-rate in a nerve fiber, thus they are iso-rate curves. The shape is described by the low-frequency slope (the slope of the tail), the Q_{10dB} (the 10dB Q of the tip, used instead of the usual 3 dB point due to the

sharpness of the tip) and the high-frequency slope. By repeating the sweep for many individual nervefibers tuned to different Characteristic Frequencies (CF), the three variables can be plotted as function of frequency. It is common practice to transform the CF of each nervefiber one octave down from cat to man, since the auditory bandwidth of cat is 40 kHz, as opposed to 20 kHz in man. Consequently, the CF values for cat must be halved to be interpreted as human CF values.

If the tuning curves are assumed to originate from a bank of linear filters, they can be interpreted as the inverse of the filter frequency response. They should thus be the result of a passive, mechanically tuned system and the shape should be independent of level. It is hypothesized by some authors that the cochlea also provides an active mechanism with negative feedback (Neely & Kim, 1983) or AGC (Lyon, 1982) to provide a sharper tuning at the tip of the tuning curve. Adaptive-Q filter models have been proposed by Hirahara and Komakine (1989) and by Kates (1991), these essentially model the same properties. The resulting tuning curves are then level-dependent and we can speak of a non-linear filterbank. This active function can be explained by active outer hair cells that are innervated from the brainstem or elsewhere in the cochlea (via efferent nervefibers) and act as motor cells to produce a displacement of the basilar membrane. Lyon's AGC-model exhibits sharp tuning when tuning curves are determined by means of pure tone sweeps, due to the AGC adapting as the stimulus frequency passes the tip of the FTC.

An average fixed frequency response (the linear component) can be more accurately determined by the reverse correlation (RevCor) method, where the impulse response of individual nerve fibers is determined using lowpass filtered noise as the input. The method has been used by Evans (1985) and many others. For a particular fiber, or CF, the input signal is constant (or slowly fluctuating), and the presumed AGC is in a stationary mode. If, however, the active section is a cochlear amplifier acting on the instantaneous signal value, the results obtained from the RevCor method should in principle be identical to those of the pure tone sweep.

The above examples illustrate that there are different measurement techniques and different theories to explain the tuning properties of the cochlea, and that there is not a single, uniform theory for the cochlear frequency selectivity.

2.3 Cochlear modeling problems.

The neurophysiological measurements yield compound data, because many elements are included between the two measurement points: tympanic membrane sound pressure and single fiber activity. The chain includes mechanical tuning in the basilar and tectorial membranes, transduction in the hair cell (mechanical-electrical conversion), active tuning mechanisms (presumably due to active outer hair cells), nerve-interconnections in the cochlea (lateral inhibition, if existing), and haircell-synapse-nervefiber connection. Derivation of the various elements in the model, including data for the design of a cochlear filterbank, becomes a very difficult task.

The neural data found in the literature, is highly variable when it comes to the shapes and slopes of tuning curves. Moreover, the data is typically based on animal measurements. The effects of hearing loss has been simulated by either causing a noise-induced loss (Liberman and Dodds, 1984) or through the use of ototoxic drugs (Harrison and Evans, 1982). A normal age-induced loss cannot easily be controlled, which is probably the reason that it was never evaluated. Modeling the normal and impaired ear, including level-dependent filter characteristics, would thus be based on a weak foundation. More consistent data are available from psychophysical measurements (see below). The same conclusion was reached by Leijon (1989), who chose a psychoacoustical model to model the impaired ear for the purpose of hearing aid evaluation. Leijon also emphasizes that the computational complexity of a physiological model with high sample rates all the way to the nerve-fibers would require many hours of computer time to process seconds of a speech signal. This problem was also evident in another cochlear model (Kates, 1991).

If a model is based on tuning curves of single nervefibers, it should ideally feature a large number of channels, perhaps on the order of 30000, similar to the number of nervefibers in the auditory nerve. This number of channels is obviously un-realistic and should for

practical purposes be limited to roughly 30-40 channels in the current study. In that case, the single-fiber analogy has little meaning, and some kind of critical-band model appears more appropriate.

2.4 Auditory models.

These models are primarily based on psychophysical measurements and are to some extent "black-box" models, in the sense that they model simple psychophysical properties, such as frequency masking, loudness growth etc. Certain aspects from the auditory physiology can be included, for example models of the hair cell.

The model described by Cohen (1989) calculates the energy in 20 non-overlapping critical bands (CB) from a 512-point FFT. The energy is then converted to loudness level (phon) by means of a histogram method over 10 seconds of speech, where estimates of threshold and uncomfortable levels are adjusted adaptively. Loudness (son) is then calculated based on Stevens' power law. Temporal effects are added, using a hair-cell model for short-term adaptation, similar to Seneff (1985).

Hermansky (1990) has proposed another model based on critical bands. The power spectrum obtained from a windowed, 256-point FFT is warped onto a Bark critical band scale and convolved by a critical-band curve given by a piece-wise linear approximation. This excitation pattern is then sampled at app. 1-Bark intervals, obtaining 18 samples (channels). To simulate an equal loudness curve, the critical band energy is pre-emphasized by an approximated frequency response, derived from normal equal-loudness contours. The last operation is a cubic-root amplitude compression, to obtain loudness in each band (specific loudness). For speech analysis, an autoregressive linear prediction analysis is performed on the loudness data from the auditory model. The model has no dynamic or adaptive effects included and according to the author, the choice of calculation models was often motivated by the need for computational efficiency.

Karjalainen (1985, 1987) has implemented a 48-channel auditory model, using FIR filters, instead of the common FFT-analysis. The power spectrum is obtained by

squaring and lowpass-filtering by a fast linear filter. A non-linear filter is then applied to simulate temporal integration and post masking. The output is converted to dB to the end result, the "auditory spectrum". A small study on just-noticeable differences (JND) of distortion indicates (Karjalainen, 1985), that it is correlated to the "auditory spectrum distance", which is the maximum difference in dB between the auditory spectrums for the unprocessed and the distorted signal. This is the only application of auditory models for sound quality measurements that has been found in the literature.

Leijon (1989) has developed an auditory model with cochlear hearing loss. This model is used for optimization of hearing-aid gain according to the proposed Loudness versus Entropy Optimization (LEO) method. This algorithm attempts to increase the estimated speech intelligibility, while keeping the total aided loudness at a pre-determined level. The main characteristics of cochlear hearing impairments, such as rapid growth of loudness, impaired auditory frequency resolution, and impaired auditory time resolution, are explicitly included in the auditory model.

2.5 Psychophysical measurements.

For the design of a filter bank, auditory filter shapes derived from psychophysical measurements must be modeled. The shape of these filters is not identical to the narrow-band noise masking pattern, one type of excitation pattern often used to characterize auditory filtering. However, the excitation pattern for a given stimulus can be derived from the auditory filter shape - the excitation pattern will be the output from an auditory filter bank as a function of filter center frequency.

The auditory filter shapes can be derived from thresholds of pure tones masked by notched-noise with varying notch width (Moore and Glasberg, 1983). The auditory filters here have Equivalent Rectangular Bandwidth (ERB) corresponding to 30 channels for the range 0.1 - 8 kHz. Glasberg and Moore (1986) provide data on normal-hearing and hearing-impaired listeners, according to a filter shape model (rounded exponential, or *roex*) described by Patterson et al (1982). Additional data on filter shapes at low frequencies for normal- and hearing-impaired listeners have been published by Peters and

Moore (1992). This data is appropriate for modeling, since analytical expressions of filter shapes are available for listeners with and without hearing loss, obtained in the same experiment. The filter parameters found by Glasberg and Moore (1986) and by Tyler et al (1984) are in some cases significantly correlated to hearing threshold, however it is pointed out, that filter characteristics may vary considerably for identical hearing losses due to individual and etiologic differences.

For the current auditory model, the question then arises, whether a representative auditory model would require masking experiments on each subject to obtain accurate estimates of filter parameters, or whether these can be derived from absolute thresholds. The current model makes a generalization, by deriving these parameters from hearing loss, which must necessarily be done if one wants to predict performance for a population. The validity of this generalization should always be regarded with caution.

The model for derivation of excitation patterns (which would be the output of an auditory filterbank) is based on the long-term power spectra of the stimulus, and temporal fluctuations, as in all speech signals, are disregarded. For an auditory model, meant for processing of real-world signals, the temporal behavior of the model is an issue to be considered.

In order to model hearing loss, level-dependent frequency selectivity and loudness in a single, coherent model, data from several studies must be combined. This also requires combining data obtained under different experimental conditions, and perhaps even with different conclusions.

3 Model description.

This section specifies the present model, which has been based on review of current literature on auditory models and psychophysics. No experimental psychophysical work was done for the development of the model. In its current state, the model represents a mixture of information from various authors, since a complete model, including hearing loss is needed. No single source has previously described such a model, except for Leijon (1989), which was not known at the time the present model was developed. There are many similarities between the two, however, Leijon has not examined the psychophysical data on which his model is based, and there is no evaluation of the model with respect to psychophysical results from the literature.

3.1 Model structure.

The emphasis in the current model is to describe the peripheral hearing function with respect to perception of sound quality, as opposed to (for instance) speech recognition. A block diagram of the complete auditory model is given in Figure 1.

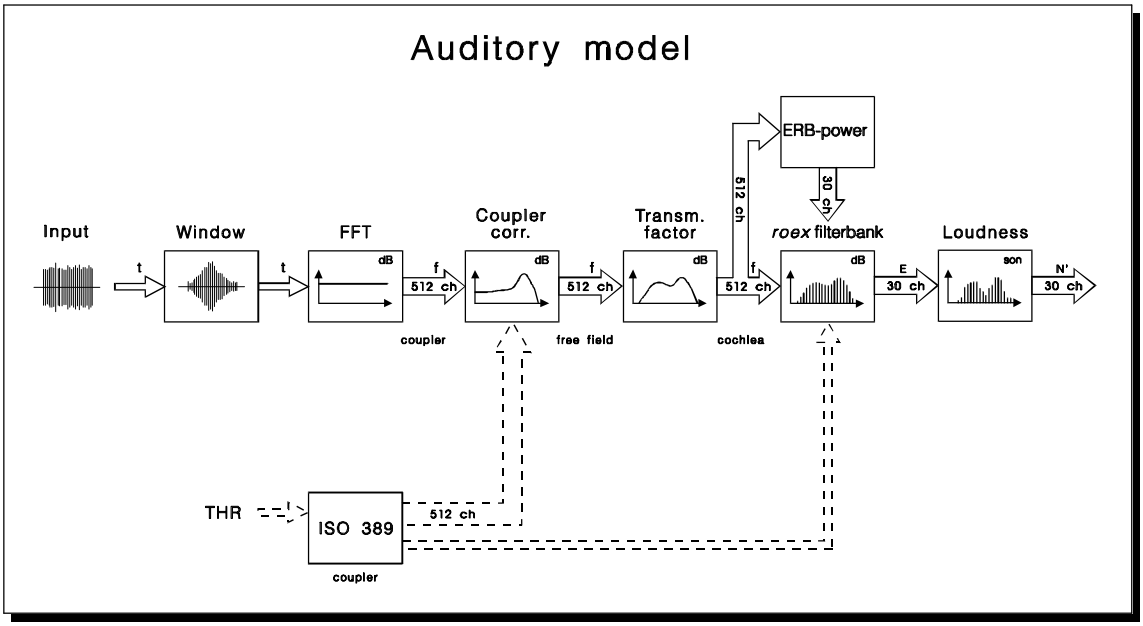

1. *Block diagram of the auditory model. Solid lines indicate signal paths, dashed lines indicate control parameters (threshold parameters for loudness initialization and to control the filter bank). See text for details.*

The current model performs the following operations on the signal:

- The incoming signal (t) is windowed to a user-specified frame-size.
- An FFT analysis is performed on the windowed signal and a power spectrum (f) is obtained.
- An equalization is then applied to the power spectrum to compensate for the frequency response of the coupler, in which the signal was recorded.
- In the same way, a transmission factor is applied by multiplication in the frequency domain. This factor can be interpreted as the linear transmission characteristics of the ear canal and the middle ear.
- The signal power is determined in 1 ERB wide bands (or wider, in the hearing-impaired case), by summing the power spectrum (f) within the limits of each band. These power values are used to adjust the filterbank:
- The resulting power spectrum is then passed through a filterbank, consisting of 30 auditory filters whose shape depend on hearing loss and on the signal power. The filter bank concept is based on work from Moore, Glasberg, Patterson and others at the University of Cambridge (see Moore & Glasberg, 1987 and Glasberg & Moore, 1990). The *roex* filterbank output, is also called the excitation pattern (E).
- The parameters for hearing loss (THR) are converted from dB HL to dB SPL and used to influence frequency selectivity in the filterbank and sensitivity in the loudness function. These initialization parameters are indicated by dashed lines.
- The *roex* filterbank output (E) is passed on to the specific loudness function that converts excitation in each channel to specific loudness, (N') according to Zwicker & Feldtkeller (1967) and Zwicker & Fastl (1990). The total loudness of an incoming signal can be calculated by summing the specific loudness across bands.

In the current configuration the auditory model represents a combination of different "schools" and experimental results from the psychoacoustical literature. In an attempt to create a coherent, practical and useful model, many compromises must be made. The literature contains disparate results and focuses on separate aspects of hearing, one model will thus not be able to unite all these results in a meaningful way. Given the large variance in research conclusions and many remaining unanswered questions, the model results should be interpreted with caution. When using the model, it should not be

considered the absolute truth, and the model output should be considered a qualitative indication, more than a quantitative measure.

The processing elements in the model are further documented in the following sections.

3.2 Power spectrum calculation.

Since the roex filter bank model is based on the power spectrum, the program must calculate the power spectrum for successive frames of the input signal. The input signal file is in the Hypersignal Workstation .TIM format, which has a 10 integer header containing information about sample rate, frame size, max. amplitude etc. The frame size and overlap between successive frames for the model is specified in a .AUD parameter text file along with other model parameters (see App. 8.1 for an example). The parameter file can be edited, using any ASCII text editor. Since the power spectrum is calculated by means of a Fast Fourier Transform (FFT), the input frame size must be a power of two in the range 2^7 - 2^{13} (128 - 8192). The overlap can be any number between 0 and frame size - 1, corresponding to a one-sample shift between overlapping windows.

After reading a frame of N samples, a Hann window is applied, using the window function:

$$W(n) = 1 + \frac{1 - \cos\left(\frac{2\pi n}{N}\right)}{2} \quad ; \quad 0 \leq n \leq N - 1 \qquad \textbf{(1)}$$

A scale factor is calculated based on the window shape to scale the power spectrum up corresponding to the power lost by applying the window.

The power spectrum is then obtained using an integer FFT and scaled to the proper floating-point value. The spectrum is scaled according to a reference signal amplitude and sound pressure level from the model parameter file to obtain the correct total acoustical power of the power spectrum.

A user-specified number of power spectra can be averaged, up to all frames of the input signal. This is useful when random signals, such as broad-band or narrow-band noise, are examined, where several spectra must be averaged to obtain stationary results.

3.3 Equalizations and coupler corrections.

The auditory model includes two types of modifications, applied to the power spectra before analysis in the auditory filterbank. The first is an equalization similar to the frequency response of the outer ear, ear canal and middle ear. The second modification is an optional coupler correction, depending on the microphone location for recording the incoming signal (free field, IEC 711 ear simulator or IEC 303 coupler).

The auditory filter bank is assumed to be preceded by a linear system that modifies the spectrum of the incoming sound (Glasberg and Moore, 1990). In a psychophysical model, this term is included to model psychophysical phenomena, such as the shape of the threshold curve and equal loudness contours, without necessarily referring to the anatomy of the ear. A physiological interpretation of the term is that it models the transfer function of hearing roughly according to the transformation that occurs from the sound in free field to the oval window of the cochlea or to the basilar membrane, due to the acoustical and mechanical systems of outer ear, ear canal and middle ear.

The threshold of hearing in free field (or MAF: Minimum Audible Field) can be interpreted as having two components (Glasberg & Moore, 1990), a fixed part affecting loudness at all levels (i.e. the parallel part of the equal-loudness contours (ISO 226, 1987)), and a level-dependent part with a different loudness growth function. The fixed part is assumed to originate from the transfer function of the outer and middle ear and should be implemented as spectrum weighting function, either as an initial filter in the time domain or as weighting of the power spectrum subsequent to FFT analysis. This correction will dominate at high levels, and could for instance model the 60- or 100-phon equal loudness contour (ELC). The remaining signal-dependent part should then account for the non-parallel equal-loudness contours and the absolute threshold curve.

The absolute threshold is implemented at a later stage in the model, namely in the loudness-coding function.

There has been some debate concerning the correctness of the standard MAF curve (ISO 226, 1987) below 1 kHz (Killion, 1978; Berger, 1981), based on evidence that the standard underestimates these thresholds by approximately 6 dB. Berger (1981) presents results that are 6 dB higher, based on 1/3-octave noise measurements in a diffuse sound field. These thresholds have been transformed to pure-tone results in free field. More recent results (ISO/TC43/WG1/N160, 1991 and Buus & Florentine, 1992) are in agreement with ISO226 (1987), thus this standard has been used in the current model. The elevated thresholds from Berger may be due to the diffuse-to-free field correction or to a different threshold criterion.

As an alternative to the ELC-based threshold corrections there is the *transmission factor*, a_0, introduced by Zwicker & Feldtkeller (1967). Meant for a binaural, free-field listening situation, the fixed frequency-dependent term, a_0, is used to model the shape of the threshold of hearing and the equal-loudness contours, above 1 kHz only. Below 1 kHz, the gain of a_0 is 0 dB, i.e. the transmission system is transparent and the threshold curve is modeled as internal (physiological) noise instead. By inspection of the equal-loudness contours (ISO 226, 1987), we see that the level-dependent effects are generally in the low-frequency range, plus some changes for high frequencies at high levels (above 7 kHz and 100 phon). The basis from which a_0 is derived is not clear, but by plotting it with the minimum audible field (MAF) data from ISO 226 (1987), it is clear that these two curves run parallel above 1 kHz. With a_0 as a fixed term in a complex model, it must be adjusted to obtain correct overall results for masking curves, equal-loudness contours, loudness growth functions etc., which is probably how Zwicker & Feldtkeller (1967) arrived at the exact shape of a_0.

The shapes of the ELC-100 curves and a_0 curves are shown in Figure 2 along with the ISO 226 (1987) curve for comparison.

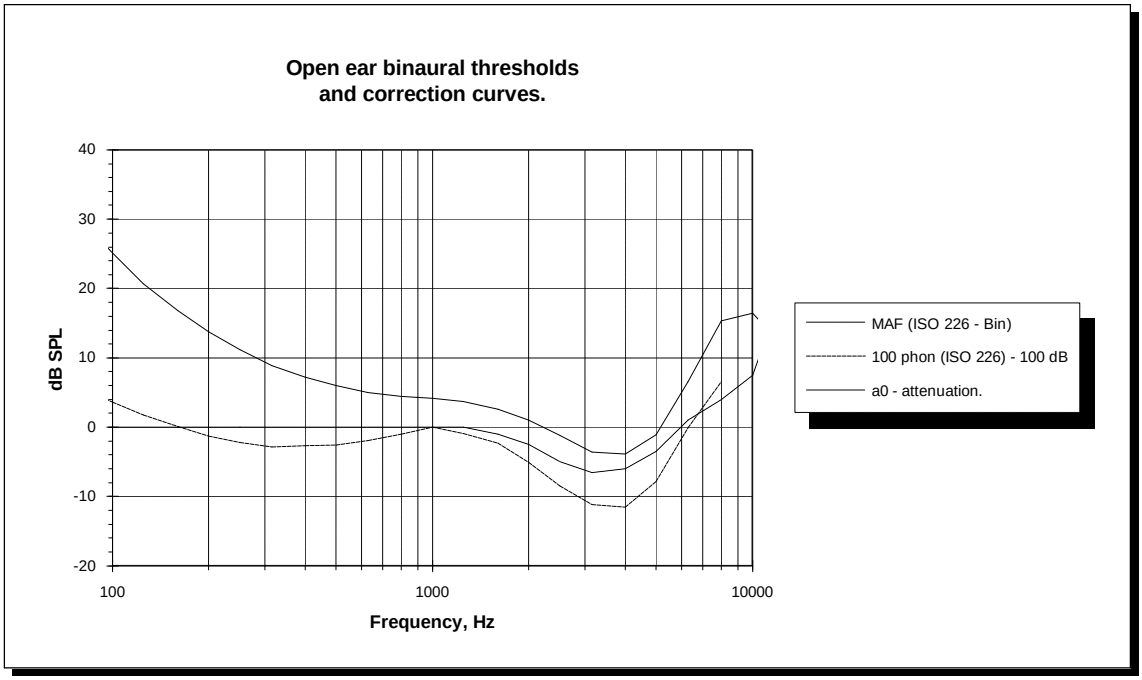

2. *Various proposed threshold correction curves. The original minimum audible field curve (MAF) and 100 phon Equal-Loudness Contour (shifted 100 dB down) are from ISO226. The a_0 curve used by Zwicker assumes that the thresholds below 1 kHz are elevated due to internal physiological noise in the cochlea, and that the transmission system itself has no attenuation below 1 kHz.*

Glasberg and Moore (1990) use different corrections, depending on the sound delivery system and the frequency range. A MAF correction is used in conjunction with a free-field listening situation or a free-field equalized headphone, whereas a MAP (Minimum Audible Pressure) correction is used with a transducer intended to produce a flat frequency response at the eardrum (Killion, 1984). Given the non-parallel equal-loudness contours, explained by the low-frequency internal noise in the cochlea, the authors recommend using the 100-phon equal-loudness contour (ELC-100) instead of MAF below 1 kHz. When used for derivation of filter shapes from notched-noise masked threshold, this correction is also found to be the most appropriate (Moore and Peters, 1990).

An important issue for model implementation is the choice of reference point, with two obvious alternatives: In the free field (at the center of the head with the listener absent) or at the tympanic membrane (TM), also referred to as the eardrum. The free field can be considered a more physically well-defined point common to all subjects, whereas the sound pressure level at the eardrum depends on individual variances in outer ear and ear

canal geometry and varying input impedance of the eardrum. The current model is intended for use with hearing aids, where signals are not presented in the free field, but rather at the eardrum or in an ear simulator (IEC 711, 1981). This points towards using the TM as reference point. However, the choice must primarily be based on the availability and reliability of psychophysical data. The largest amount of coherent data is provided in the ISO 226 (1987) standard for normal-hearing subjects, listening binaurally. Here, MAF data and equal-loudness contours are given for pure tones, and these are used in the auditory model.

In the auditory model, the auditory thresholds for a subject are input as dB HL values from the audiogram, as obtained on an IEC 303 (1970) coupler in standard audiometry. These hearing level values are then converted to dB SPL (ISO 389, 1991) in the coupler and then to equivalent free-field values, using the IEC303 - free field corrections provided by Bentler and Pavlovic (1992). For a binaural listening situation, a threshold correction must be subtracted. Killion (1978) suggests a monaural disadvantage of 2 dB, while Berger (1981) suggests 3 dB. From a signal detection point of view, and assuming that the threshold of hearing is equivalent of a noise floor and that the noise sources of the two ears are uncorrelated, two detectors are equivalent to a 3 dB increase in signal-to-noise ratio, and a corresponding drop in threshold value. Bentler and Pavlovic (1989) use 1.5 dB at low frequencies, rising to 2.5 dB and 3.8 dB at 5 and 6 kHz, respectively. In the current project it was decided to use a 3 dB flat correction, as was also proposed by Scharf & Buus (1986), e.g. the binaural threshold power equals half the monaural threshold power. At higher levels, power summation is not the important factor, but rather loudness summation, so the monaural-binaural correction must be made in the loudness domain (see section 3.5.1). In either case, the binaural model assumes two completely identical ears, and the asymmetrical case is not accounted for.

As previously mentioned the output from a hearing aid is typically recorded in an ear simulator (IEC 711, 1981), where the sound pressure level at the microphone represents the level at the eardrum in an average ear. Consequently, this type of signal must be weighted by a coupler correction frequency response, transforming it to equivalent free-field values. The open-ear transfer function - from free-field to eardrum - has been

measured by Shaw (1974) and later presented in numerical form by Shaw & Vaillancourt (1985). By subtracting Shaw's gain values from to the IEC 711 coupler spectra, the equivalent free-field spectra are obtained as input to the model.

The MAF curve has a prominent dip from 1 to 8 kHz with a minimum at 4 kHz, which is logically assumed to arise from the acoustic gain of the external ear and in particular the ear-canal resonance. However, the open-ear transfer function (Shaw, 1974) has its peak located at 2.6 kHz. By adding Shaw's data to the MAF curve, a threshold curve for the sound pressure level at the tympanic membrane can be obtained. This is termed Minimum Audible Pressure (MAP). Killion (1978) has derived MAP from MAF in this manner. The MAP curve is not flat as would be assumed from the above hypothesis, but exhibits a "hump" at 2500 Hz, where the open-ear transfer function is located. No clear explanation for this hump has been offered by Killion, who suggests the eardrum-to-basilar membrane transfer function as an explanation.

Another investigation of the open-ear transfer function (Mehrgardt & Mellert, 1977) shows a broader peak around 3-4 kHz which is in better agreement with the dip in the MAF curve. By adding MAF and this open-ear response, a somewhat smoother MAP curve is obtained, with a dip at 1-1.25 kHz as the most prominent feature. This frequency, is where the middle ear begins to attenuate the signal (Allen, 1985), which could account for the sharp rise in the MAP curve beyond 1.25 kHz.

It turns out that most MAP data published in the literature are essentially derived from the ISO 226 (1987) MAF data or other MAF measurements, based on an average free-field to eardrum transfer function. The current model should therefore use the free-field as reference, with three choices of equalization curves:

- The a_0 correction used by Zwicker & Feldtkeller (1967) and Zwicker & Fastl (1990).
- The ELC-100 curve as proposed by Glasberg & Moore (1990).
- A combination of the two, where the ELC-100 curve is modified below 1 kHz to be flat.

When the model is then used with reference to the eardrum, or an IEC 711 ear simulator, two MAF-MAP corrections are available:

- Shaw and Vaillancourt (1985), based on Shaw (1974).
- Mehrgardt & Mellert (1977).

It is also possible to convert signals recorded in an IEC303 (6 cm^3) coupler, using the 6 cm^3-free-field transformation proposed by Bentler and Pavlovic (1992).

3.4 Auditory filter bank.

The filter model originates from the work by Patterson, Moore, Glasberg and others (Patterson et al, 1982; Moore & Glasberg, 1983, Tyler et al, 1984; Glasberg & Moore, 1986; Moore & Glasberg, 1987; Glasberg & Moore, 1990). The auditory filter model is based on detection of pure-tone signals in symmetrical and asymmetrical notched-noise maskers. The derivation of the filter shape is based on two assumptions: 1) The auditory filter used for detection of the signal in the masker will be centered at the frequency yielding the highest signal-to-masker ratio; 2) Detection threshold corresponds to a fixed signal-to-masker ratio at the output of the filter, known as detection efficiency. Under these assumptions, an analytical expression for the shape of the auditory filter can be derived. The parameters in the filter expression can be determined for an individual by means of the notched-noise masked thresholds.

Based on the auditory filter shape, excitation patterns for harmonic stimuli can be calculated as the output of each filter in a filter bank (Moore & Glasberg, 1987). This calculation model centers an auditory filter at each frequency component in the stimulus. For implementation of a generalized auditory model, this concept must be modified, to limit the number of channels and to obtain an acceptable processing speed. On the other hand, a model with few filters at fixed center frequencies violates the first assumption of the auditory filter model. The model should ideally focus on local or global peaks in the power spectrum, or perhaps on local peaks in pre-defined frequency regions. Using this

approach, the entire auditory spectrum would be covered, while the auditory filters were allowed to maximize signal-to-masker ratio locally[1].

However, for convenience and subsequent interpretation by a neural network, the current model uses a fixed number of channels at fixed center frequencies. When the filter bandwidth increases as function of hearing loss (section 3.4.1) and level (section 3.4.2), the filters become overlapping, which is not a correct interpretation of the auditory system. It should rather be modeled by a decreasing number of non-overlapping filters. This is discussed further in section 3.5.2, and a correction for the widening filters at fixed center frequencies is introduced.

The auditory filter shape W(g) is generalized by the function (Moore & Glasberg, 1986):

$$W(g) = (1-r)(1+pg)e^{-pg} + r \qquad \textbf{(2)}$$

This is the rounded exponential, *roex(p,r)*, filter, with two parameters, the exponential slope parameter, *p*, and the base level *r*. A high *p* indicates sharper tuning, and *p* is affected by frequency, level in the band and by hearing loss. A typical value at 1 kHz and low input levels for a normal-hearing listener is 20 - 25. The second parameter, r determines the filter weight outside the passband, the stopband level. This is often highly correlated to absolute threshold of hearing. *g* is the normalized distance from the center frequency of the filter, f_c.

$$g(f) = \frac{|f - f_c|}{f_c} \qquad \textbf{(3)}$$

The filter function, *W(g)*, can also be thought of as a weight function applied to the power spectrum of the stimulus. An example of the filter function is shown in Figure 3.

[1] Since the spectrum of signal and masker cannot be estimated independently, we make the assumption that a filter centered on a spectral peak yields the highest signal-to-masker ratio.

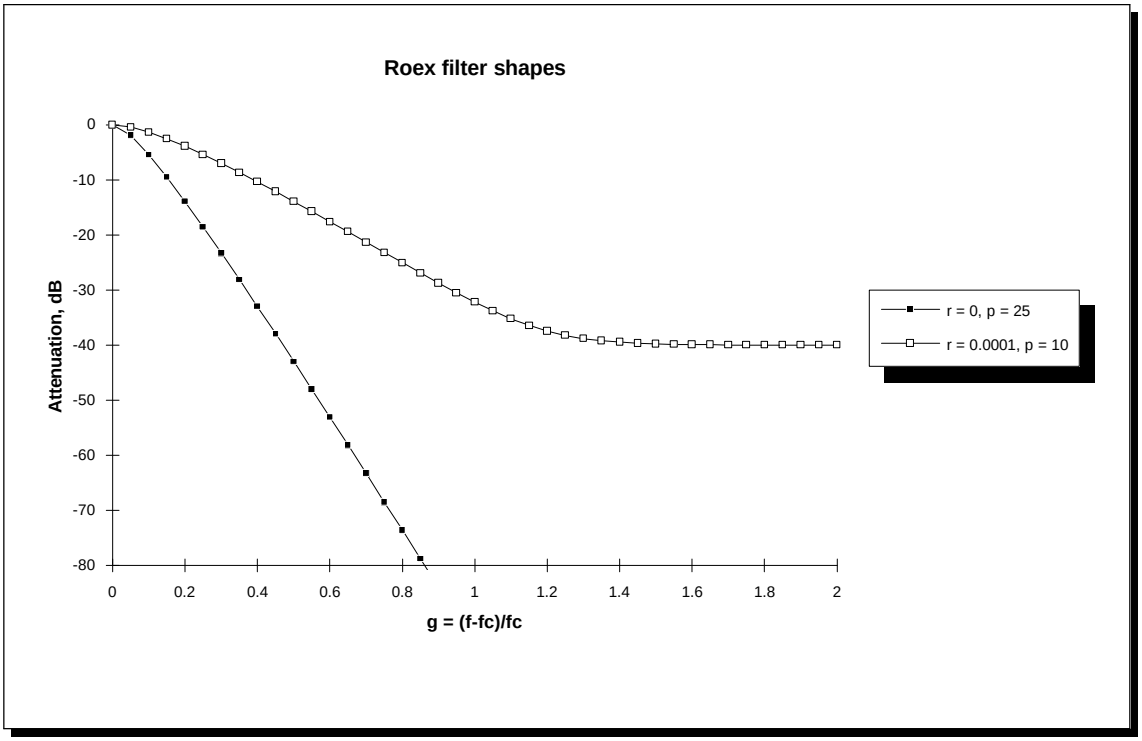

3. *Sample plots of roex(p,r) filter shapes with different slopes, p, and tails, r.*

The "tails" of the filter, characterized by *r*, appear to be linked to the absolute threshold of hearing (Glasberg & Moore, 1986) and are thus omitted from the filter bank stage, since the threshold function will be implemented in a later stage of the auditory model. The simplified *roex*(p) filter equation used here is:

$$W(g) = (1 + pg)e^{-pg} \qquad \textbf{(4)}$$

The *p* parameter determines the slopes of the filter and thus indirectly the bandwidth. For moderate sound levels, the filter shape becomes asymmetrical, and *p* is allowed to have different values on the two sides of the center, p_l below f_c and p_u above f_c. When viewed on a linear frequency scale for constant p, the roex filters are symmetrical with a widening bandwidth as center frequency increases. Viewed on a logarithmic frequency scale, the filters are all the same width and asymmetrical. This is illustrated in Figure 4.

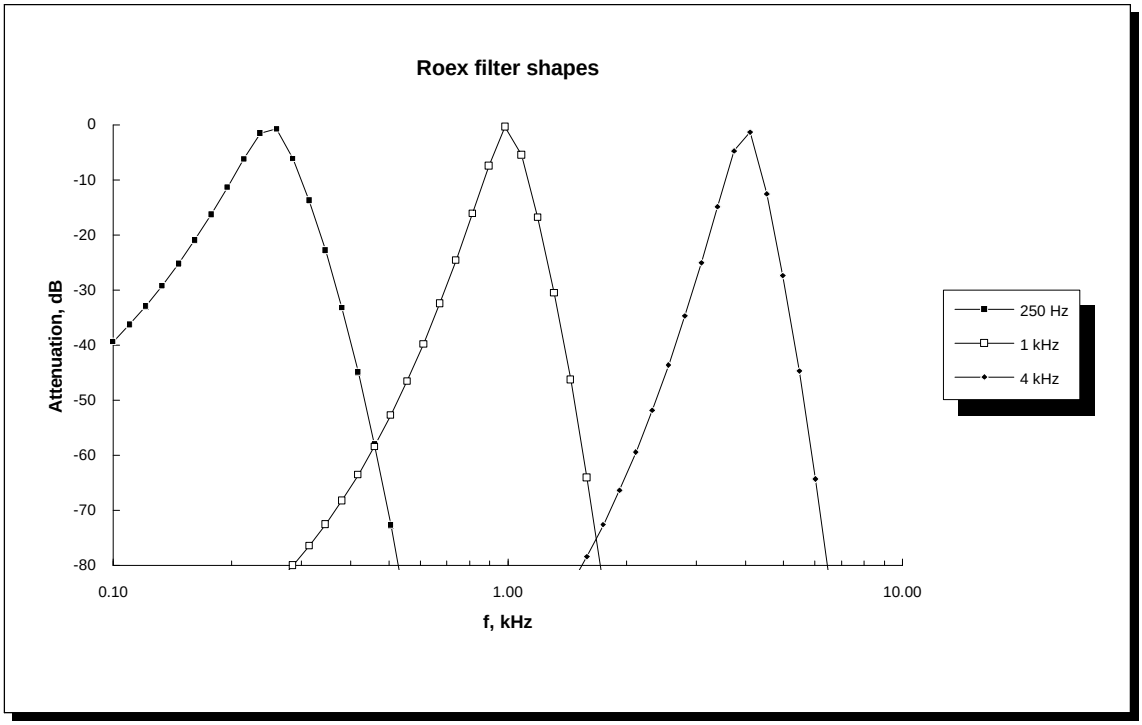

4. *Examples of three typical roex filter shapes at three center frequencies. The p values are the same above and below the center frequency.*

A digital filter model with logarithmically spaced center frequencies will thus be more suited than an FFT-model with linearly spaced lines. The *roex* filter can be approximated by a "gamma-tone" impulse response, as Moore et al (1989) have done in a paper on temporal gap detection. This impulse response exhibits amplitude and phase response similar to those derived from single neuron measurements in the cat. The result is a fixed filter, independent of the signal power in that band, contrary to the general theory, that auditory filters cause increased upward spread of masking with increasing level (Lutfi & Patterson, 1984).

As an alternative and future improvement to the FFT-approach, a wavelet-based filterbank with center-frequencies and bandwidths corresponding more closely to a critical-band scale (Agerkvist, 1992) or an ERB-scale might be more correct. Such a pre-processor would have high temporal resolution at high frequencies and low temporal resolution (i.e. a long window) at low frequencies, as the auditory filterbank does, when modeled as a series of simple resonators (de Boer, 1985).

The FFT-based model initially determines the power spectrum and subsequently corrects the spectrum for external and middle ear transfer functions, as discussed in section 3.3. Based on this corrected spectrum, which can be interpreted as the input spectrum to the cochlea / filterbank, the parameters of the auditory filters can be adjusted. The adjusted filters are then easily applied to the signal by multiplication in the frequency domain. A disadvantage of the FFT-based model is the limited time resolution due to a block-based analysis. With a sampling rate of 20 kHz, the time window is 12.8 and 25.6 ms for a 256- and 512-point FFT, respectively. A short-time FFT will also provide very poor frequency resolution, wider than 78 and 39 Hz for the 256- and 512 point FFTs, respectively. The degree of smearing in the frequency domain also depends on the choice of window function.

Furthermore, phase information and time delays are not similar to a real ear, where a cascade of IIR filters would provide a more realistic model due to the basilar membrane traveling wave simulation (Lyon, 1982). Recent data (Moore & Glasberg, 1989) indicate that the ear cannot detect phase shifts of single component in a harmonic stimulus when phases of the components were randomized. For a speech signal it is likely, that the power spectrum provides the major speech cues (Leijon, 1989), thus the loss of correct phase information in a power spectrum method is acceptable. In the case of other signals, phase sensitivity may be a concern, but the knowledge in this area is still limited. Other power-spectrum-based methods are described by Cohen (1989) and Hermansky (1990) - see section 2.4 for a summary.

Moore and Glasberg (1983) presented data from several authors on the equivalent rectangular bandwidth (ERB) of the auditory filter as function of frequency in the range 0.1 - 6.5 kHz. These data were later extended (Glasberg and Moore, 1990) to cover the range 0.1 to 10 kHz.

The ERB can be calculated as:

$$ERB_{Hz} = 24.7(4.37f_c + 1) \qquad \textbf{(5)}$$

where ERB is the bandwidth in Hz, and f_c is the center frequency of the auditory filter in kHz. Based on this, a psychoacoustical scale, similar to the Bark scale (Zwicker & Feldtkeller, 1967), has been derived by integrating the reciprocal of the critical-band function. The ERB-rate, or E scale is related to frequency by:

$$E = 21.4 \log(4.37f + 1) \qquad \textbf{(6)}$$

where f is in kHz.

The inverse expression for calculating f as a function of E is:

$$f = \frac{10^{\left(\frac{E}{21.4}\right)} - 1}{4.37} \qquad \textbf{(7)}$$

Thus, an auditory filter bank with fixed center frequencies should have these evenly distributed on an E-scale. The E-scale is valid in the range E = 3 to 35, corresponding to center frequencies from 87 Hz to 9.65 kHz. This range should then be covered by 33 filters, for a fixed-center-frequency model, an appropriate channel number for subsequent data processing by an artificial neural network. In order to model masked thresholds for broad-band, white noise signals adequately, 2 channels/ERB are required (Buus, 1992), i.e. 65 channels, but this will increase the complexity of the system and probably result in a high degree of correlation between channels.

3.4.1 Filter shape as a function of level.

The low-frequency slope of the roex filter depends on the signal level in each band being added to the filter output. With increasing signal level, the lower branch becomes more shallow for normal-hearing subjects. By analyzing data for asymmetric notch-noise maskers from several studies and collapsing these across center frequencies, Glasberg & Moore (1990), have determined the following linear relationship between the slope

parameter p_l below center frequency and the sound pressure level X, corrected for external and middle ear transfer functions (section 3.3), in the band:

$$p_l(X, f_c) = p_{l(51, f_c)} - 0.38 \frac{p_{l(51, f_c)}}{p_{l(51, 1k)}} (X - 51) \quad \textbf{(8)}$$

where $p_{l(51,fc)}$ is the value of p_l at that center frequency obtained at 51 dB SPL/ERB, and $p_{l(51,1k)}$ is the value of p_l at 1 kHz and a noise spectrum level of 30 dB SPL/Hz, corresponding to 51 dB SPL/ERB at 1 kHz. The value of $p_{l(51,fc)}$ depends on the center frequency, f_c, and is calculated from the ERB, remembering that $p_{l(51,fc)} = 4f_c/\text{ERB}$, where f_c is in Hz. The valid range of levels for this equation is not clear, however one of the cited studies (Lutfi & Patterson, 1984) has obtained data for spectrum levels from 20 to 50 dB SPL/Hz, corresponding to 41 - 71 dB SPL/ERB at 1 kHz. The data from these studies has will not be presented separately in here, since the equation presented by Moore and Glasberg (1987) includes unpublished data, and the level dependency function thus relies on the final analysis in the follow-up paper by Glasberg & Moore (1990).

The slope parameter above center frequency, p_u, does not vary consistently with level (Moore and Peters, 1990), but only with center frequency f_c and equivalent rectangular bandwidth, ERB:

$$P_u(f_c) = 4000 f_c / ERB \quad \textbf{(9)}$$

where f_c is in kHz and ERB is in Hz. The model for calculating filter shapes thus determines the power in bands that are one ERB wide (eqn. 4) and subsequently sets the filter slopes according to eqn. 8 and 9. For a high signal level in a band below center frequency, the low-frequency slope widens, and will be weighted higher in calculating the output of that *roex* filter. For a stationary stimulus, the effective response of a filter at higher center frequency will have local peaks, where high-level components are, as shown in Figure 5. This filter response does seem contrary to normal masking theory, assuming monotonous filter functions. However, the significant feature of the model, the

derived excitation patterns generally assume the correct shape as indicated in Figure 13, section 4.2.1.

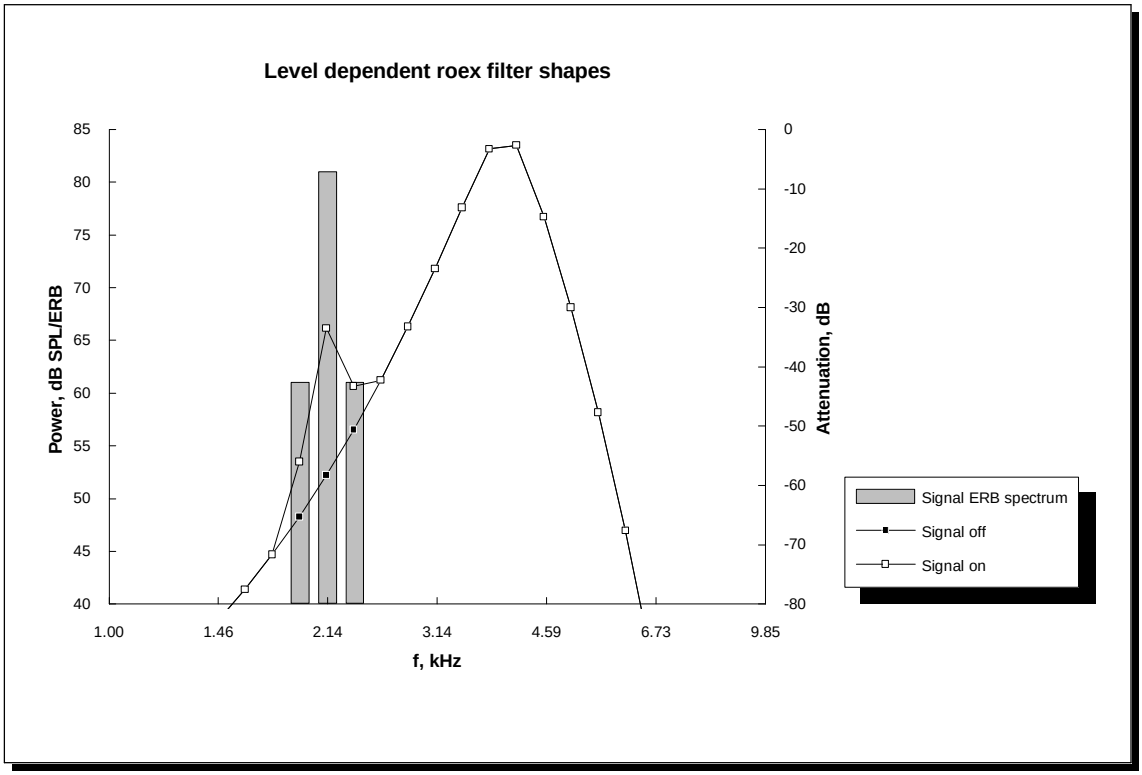

5. *Effective roex filter shape at 4 kHz, when a 1 kHz pure tone signal is applied. The signal decreases the filter slope, and is thus weighted higher. The resulting excitation patterns exhibit increased upward spread of masking with increased level.*

Since filter shape depends on the power passing through that filter, it might seem obvious that the correct procedure for calculating the filter shape would be a series of iterations, where the output power and the filter shape interacted. This would be a feedback arrangement of filter shape and output power, as opposed to a feed-forward model, where the input power is used to set the filter shape of the *roex* filter. Both assumptions have been tested by calculating the excitation patterns for a 1 kHz sinusoid at a range of levels (Moore & Glasberg, 1987), whereby only the input model (feed-forward) produced the correct excitation patterns with increasing upward spread of masking. For broad-band signals, on the other hand, strong components far from a given filter should not be able to affect its shape, and an extension is proposed, where the input power in one rectangular band, 1 ERB wide, is used to calculate the shape of that

particular filter channel. The calculation algorithm is listed in a FORTRAN program (Moore & Glasberg, 1987), which was duplicated in the current model.

The level-dependent filter shapes are for normal-hearing subjects only. Since data were collapsed to 1 kHz, the model is also based on the assumption that filter shape varies with level the same way across all center frequencies. The authors emphasize, that more data is needed to test this assumption.

Figure 12 (section 4.2.1) shows examples of excitation patterns from the model (i.e. filter bank output) for various pure tones.

3.4.2 Filter shape as a function of hearing loss.

Glasberg & Moore (1986), measured auditory filter shapes for listeners with unilateral and bilateral cochlear hearing impairments and found ERB and p_l to be significantly correlated with hearing threshold in dB SPL (on a B&K 4153/IEC 318 artificial ear) for a 1 kHz pure tone stimulus. Additional data, including other frequencies, have later been reported by Peters and Moore (1992) and Stone (1992). The data include unilateral and bilateral losses of mixed origin (noise, presbycusis). In the current report, a model for the filter shapes as function of cochlear (sensorineural) hearing loss has been determined, based on further analysis of the published data.

Glasberg & Moore (1986) found that the equivalent rectangular bandwidth (ERB) in impaired ears increased for thresholds above 30 dB SPL, based on measurements at 1 kHz. With inclusion of additional data and by transforming all ERB values to a 1 kHz equivalent, the data points for 137 filters on 50 ears can be plotted. This is shown in figure 6.

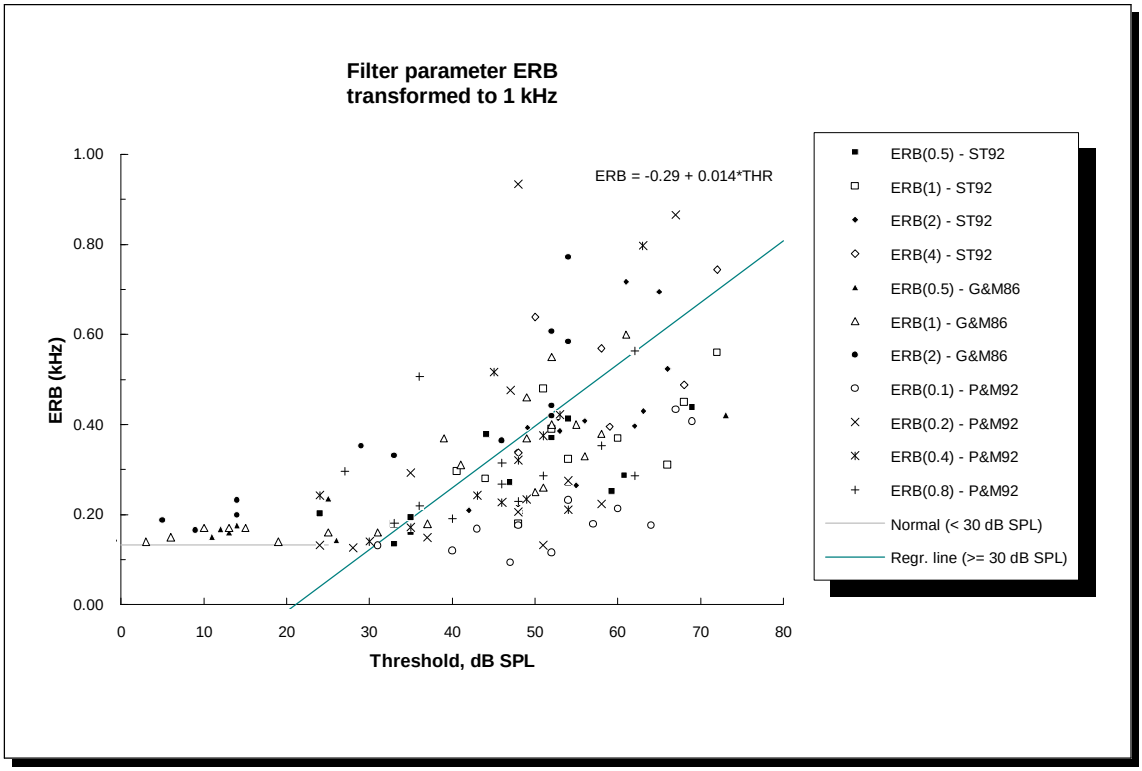

6. *Equivalent rectangular bandwidth (ERB) plotted as a function of auditory threshold in dB SPL. The data originate from Glasberg & Moore (1986), Peters and Moore (1992) and Stone (1992). All values have been transformed to equivalent ERB at 1 kHz center frequency. The 0.1 and 0.2 kHz data were excluded prior to the regression analysis (see text).*

It is clear, that there is a large spread of ERB values for a given threshold. As a simple approximation and generalization, the current auditory model should predict the rectangular bandwidth based on thresholds. Following the argument from Moore & Glasberg (1986), that auditory filters are normal for thresholds below 30 dB SPL, a linear regression analysis was performed on all data points above 30 dB SPL. At 0.1 and 0.2 kHz, however, the ERB-values are very scattered. The derivation of these filter shapes is very sensitive to the low-frequency transfer characteristics of the transducer, and show a large spread, even for normal-hearing listeners (Moore & Peters, 1990). This is consistent with physiological results, showing that the low-frequency tuning curves are very broad and poorly defined below app. 600 Hz in cats, corresponding to 300 Hz in humans (Evans & Elberling, 1982). The 0.1 and 0.2 kHz data points were thus excluded from the analysis.

A linear regression analysis for thresholds above 30 dB SPL, excluding 0.1 and 0.2 kHz data points, yields the following relationship at 1 kHz:

$$ERB_{1k}(THR) = -0.29 + 0.014 \& THR \;;\; THR \text{ m } 30.7 \text{ dB SPL} \quad \textbf{(10)}$$

for thresholds in the range 31 to 70 dB SPL. Above this range, there is no data for prediction of filter shapes, and practically no remaining frequency selectivity (Ludvigsen, 1985). Below this range the ERB is normal as expressed in eqn. 5 with correction for level (see below). The regression analysis is similar to the analysis of Glasberg & Moore (1986), who found a more shallow slope (0.0097). There is a modest and significant correlation (r = 0.52, p < 0.0001), so the linear model was accepted. The ERB here is expressed as proportion of center frequency, which at 1 kHz is equal to the filter bandwidth in kHz.

The data might be better fit with a power- or exponential function, thus providing a smooth transition from normal hearing to hearing loss. Furthermore, a data transformation might provide a more constant spread of Y-values with increasing threshold. For simplicity, however, a linear model was used in this and the following analyses on change in filter shapes with threshold in dB SPL. This also allows for a straightforward and meaningful introduction of level effects into the model, since the level effects are also linearly dependent of dB SPL (section 3.4.3).

Consistent with summarized results from several studies (Tyler, 1986) auditory filters broaden with increasing hearing loss, but there is a large spread around the general trend. An alternative would be to specify the filter parameters on an individual basis, but this is not included in the current implementation of the model. The regression suggested above is always used. Leijon (1989) specifies typical values for widened filters for his model, but it is unclear how these values are then interpolated between test frequencies for each filter channel. His model is only used with a number of hearing loss cases and not for any audiogram.

For the LF-slope (high-pass) as a function of threshold, p_l, a scatter plot is shown in Figure 7. There are certain data points that clearly do not fit the trend of decreasing

slope with increasing threshold. These are primarily data for low center-frequencies (100, 200 Hz), where the filter fitting procedure tends to show larger variation across individuals and is furthermore very sensitive to the type of threshold correction used (Moore et al, 1990). The remaining data points can be approximated by a similar piecewise linear function.

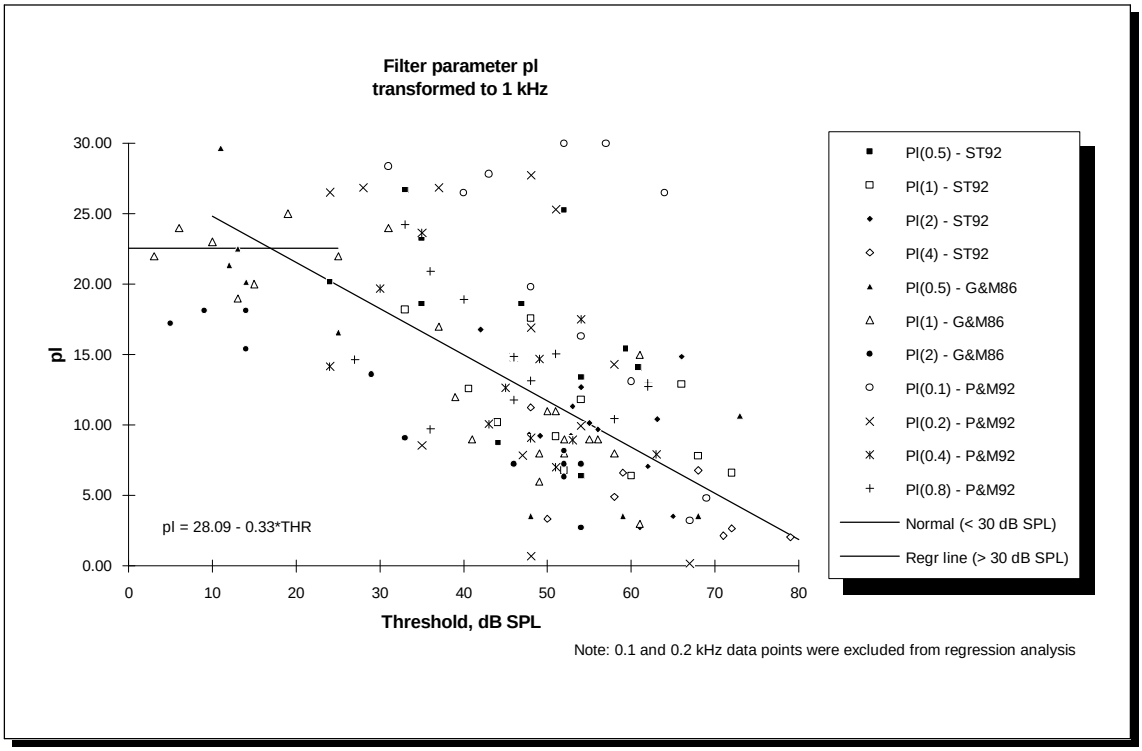

7. *The low-frequency filter slope parameter, p_l, plotted as a function of auditory threshold in dB SPL. The data originate from Glasberg & Moore (1986), Peters and Moore (1992) and Stone (1992). All values have been transformed to equivalent values at 1 kHz center frequency. The regression line was calculated after exclusion of the 0.1 and 0.2 kHz data, that showed very large spread.*

Based on these selection criteria and using only points with thresholds above 30 dB SPL, a regression analysis for p_l transformed to 1 kHz yields:

$$p_l(1k, THR) = 28.09 - 0.33 \& THR \;;\; THR \geq 16.9 \text{ dB SPL} \qquad \textbf{(11)}$$

for thresholds in the range 16.9 to 70 dB SPL. No predictions are made above this range. Since ERB, p_l and p_u are related (Glasberg & Moore, 1990), the regression analysis should indicate intersections for identical threshold values (30.7 resp. 16.9 dB SPL). The large spread of data points indicates that they could, in fact, intersect at the

same point, but without clear evidence, no modification of the analysis results was made. The filter slope decreases with increasing hearing loss ($r = -0.61$, $p < 0.0001$). This is consistent with the increasing ERB and furthermore leads to an increased upward spread of masking (Tyler et al, 1984). A similar shallower slope on the low-frequency side of psychoacoustical tuning curves has been observed by Florentine et al (1980). Even though the model fitting was done without the 100 Hz and 200 Hz data points, it has been extrapolated to cover these frequencies, based on the remaining data points.

For the HF-slope (low-pass) as a function of threshold, pu has also been plotted as a function of absolute threshold, as shown in figure 8. This plot has considerable scatter, and no clear trend is evident.

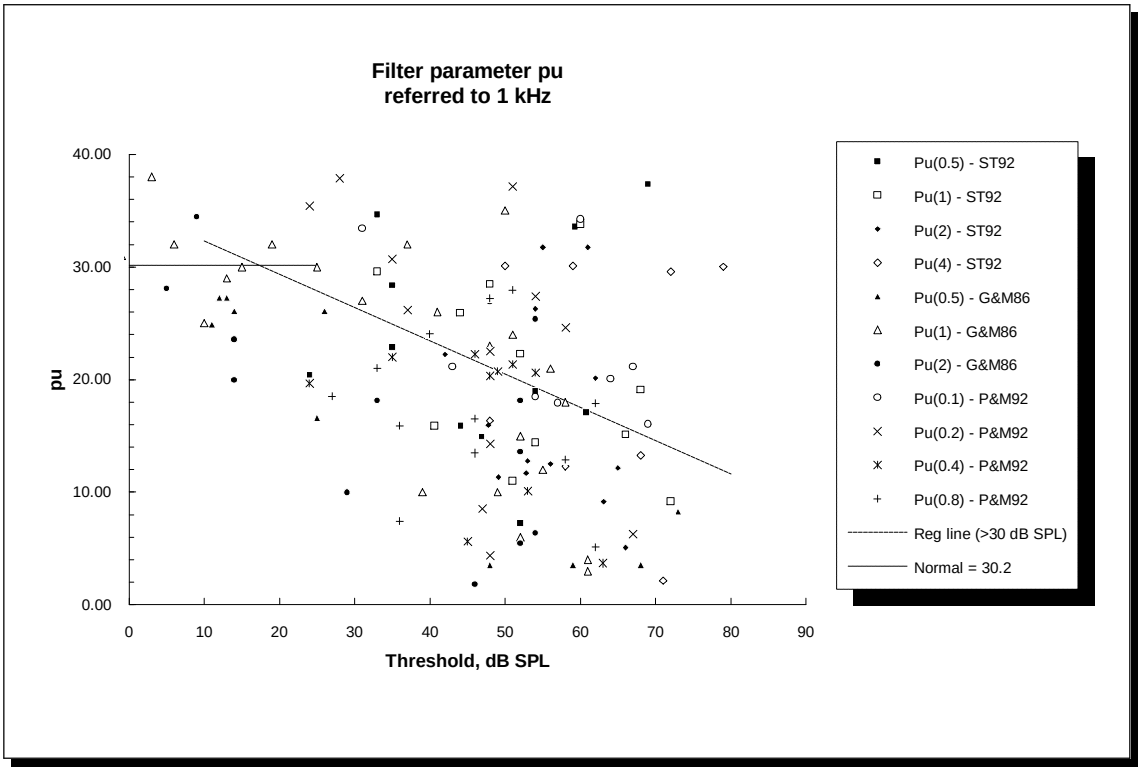

8. *The high-frequency filter slope parameter, p_u, plotted as a function of auditory threshold in dB SPL. The data originate from Glasberg & Moore (1986), Peters and Moore (1992) and Stone (1992). All values have been transformed to equivalent values at 1 kHz center frequency.*

There seems to be a weak tendency of a decreasing slope with increasing hearing loss corresponding to increased downward spread of masking with level, although the data show a dubious correlation ($r = -0.36$, $p < 0.08$) for thresholds above 30 dB SPL. In line

with this result, Florentine et al (1980) found no systematically increasing downward spread of masking with hearing loss. Due to the filter-fitting process, the value of p_u is not well defined when the value of pl is much smaller (Glasberg & Moore, 1986), which can serve as a partial explanation of the large spread of data points.

Based on these considerations, the value of p_u was kept constant (= normal hearing) in the model, and only increased upward spread of masking with hearing loss was included.

The auditory filter shape in hearing-impaired subjects may be highly variant, even normal auditory filter can be found (Tyler, 1986). The data used for the present analysis show significant spread. However, the present model is accepted as a reasonable approximation with interpolation of filter shapes to other frequencies. A correction was required, since all thresholds in the original data were expressed as absolute thresholds in dB SPL on a B&K 4153 artificial ear (IEC 318). The audiogram, expressed in dB HL was thus converted to dB SPL using ISO389 (1991) for the IEC 318 coupler.

3.4.3 Filter shape as a function of level and hearing loss.

In the current auditory model, the level and hearing loss effects mentioned above should be combined in a meaningful way, that corresponds with experimental results.

In section 3.4.1 filter shapes as function of level for normal-hearing listeners were discussed. Since no similar data has been published for hearing-impaired listeners, the initial assumption is to add the two effects in some fashion. Florentine et al (1980) conclude that cochlearly impaired listeners show reduced frequency selectivity compared to normal listeners at equal absolute levels (dB SPL). The masking model described by Ludvigsen (1985) demonstrates decreasing masking slope with increasing level. The masked threshold is then further modified by hearing loss, i.e. level and hearing loss (< 70 dB HL) are both leading to reduced frequency resolution.

A recent investigation by Dubno and Schafer (1992) led to a similar result. In their study the absolute thresholds of hearing impaired subjects were simulated in normal-hearing subjects by means of a shaped broad-band noise. The masked thresholds obtained with

both a notched-noise masker and a narrow-band masker were measured at identical Sensation and Sound Pressure Levels due to the simulated hearing loss. Under these equal conditions, the hearing-impaired subjects still had reduced frequency selectivity. From the notched noise masked thresholds, *p* (assuming symmetric filters) and ERB values were derived (Patterson et al, 1982) - with *p* values below those of the simulated hearing losses, and ERB values were similarly higher than for the masked normal-hearing listeners. For the hearing-impaired listeners, the presented graphs indicate that masked threshold slopes decrease with increasing level, however this is not discussed in the paper, and the level effect in hearing-impaired listeners may be dubious.

The first level and loss effect, **Alternative 1**, is that the model should combine the effects of level and hearing loss, even at high levels. The level dependency effect for p_l (Glasberg and Moore, 1990) is based on a masker spectrum level of 30 dB SPL/Hz (51 dB SPL/ERB at 1 kHz), whereas the hearing loss effect is based on a spectrum level of 50 dB SPL/Hz (71 dB SPL/ERB at 1 kHz). The regression line is essentially the same, but levels are referred to 71 dB SPL/ERB instead. Furthermore the values are modified by frequency. Combining all of this, we get a set of equations, where ERB is the equivalent rectangular bandwidth in kHz, f_c is the band center frequency in kHz, X is the sound pressure level in one E band, and THR is the audiogram threshold in dB SPL, measured in an IEC 318 artificial ear:

$$ERB(f_c, THR) = \frac{4.37 f_c + 1}{5.37}(-0.29 + 0.014 \,\&\, \max(30.7, THR)) \qquad \textbf{(12)}$$

For the low-frequency slope, p_l, as function of frequency, level and hearing loss, the formula for Alternative 1 becomes:

$$p_l(f_c, X, THR) = \frac{5.37 f_c}{4.37 f_c + 1}(28.09 - 0.33 \,\&\, \max(16.9, THR) - 0.38(X - 71)) \qquad \textbf{(13)}$$

Based on the vague results on level and loss effects on the high-frequency slope parameter, p_u, it was decided to make it a function of center frequency, f_c, only:

$$P_u(f_c) = \frac{161.94 f_c}{4.37 f_c + 1} \qquad \textbf{(14)}$$

It was decided to limit hearing thresholds to 70 dB SPL, and levels to the range 20 - 100 dB SPL/ERB, since psychophysical data is not available outside of these ranges. The auditory model assumes constant values outside the ranges equal to the values at the limits.

Alternative 2 assumes level dependency only at normal hearing (here defined as thresholds below 20 dB SPL, the cutoff-point for the p_l regression curve). Here, the level and threshold effects have been combined in a more logical way: There are no level effects at thresholds above 20 dB SPL. For lower thresholds, the tuning is increased with decreasing levels, down to a cut-off point, which depends on threshold. This means that for a normal hearing threshold, there is a 20 dB range at the bottom with increasing tuning, similar to a fully functional cochlear amplifier. This is shown schematically in figure 9 for a number of hearing losses. Below 51 dB SPL/ERB, there is no further increase in filter slope. In this manner, the tuning enhancement is active only at low levels combined with little or no hearing loss. The combination of effects was done by using the intersect and slope values corresponding to the level effect, with only a slight decrease in goodness of fit. The effect presented here shows sharper tuning when the hearing thresholds are normal (< 20 dB SPL) and the signal power is low, as was also reported by Peters and Moore (1992).

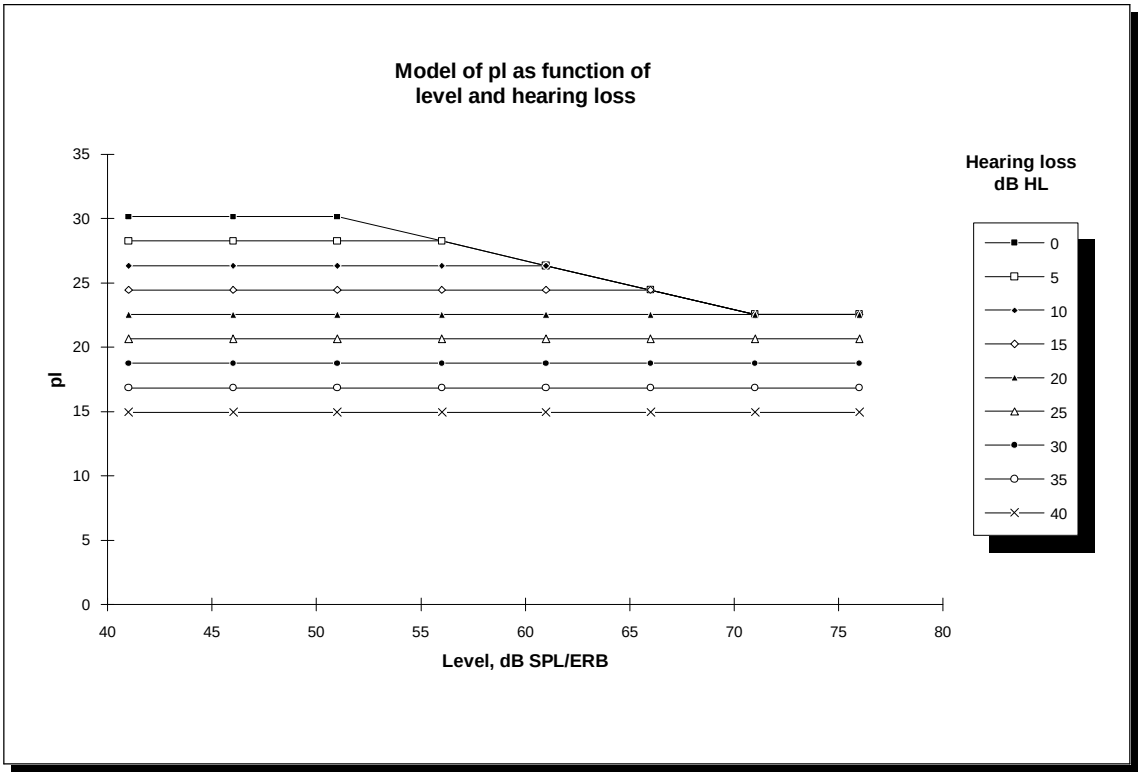

9. *Schematical representation of the level dependent increase in filter slope for low thresholds (< 20 dB SPL) and low levels (< 71 dB SPL/ERB) as described in Alternative 2. For normal hearing, the bottom 20 dB show increased tuning with decreased levels.*

The formula for Alternative 2 is:

$$p_l(f_c, X, TH) = \frac{5.37 f_c}{4.37 f_c + 1}\left(30.16 - 0.38 \cdot (\max(\min(0, X - 71), TH - 20) + 20)\right) \quad \textbf{(15)}$$

The approach used to modify and fit this alternative was not to use an empirical statistical procedure, such as multiple regression, but rather to carefully modify the known models (Moore and Glasberg, 1987 and Glasberg and Moore, 1990), hereby preserving the larger bulk of data and knowledge that has evolved.

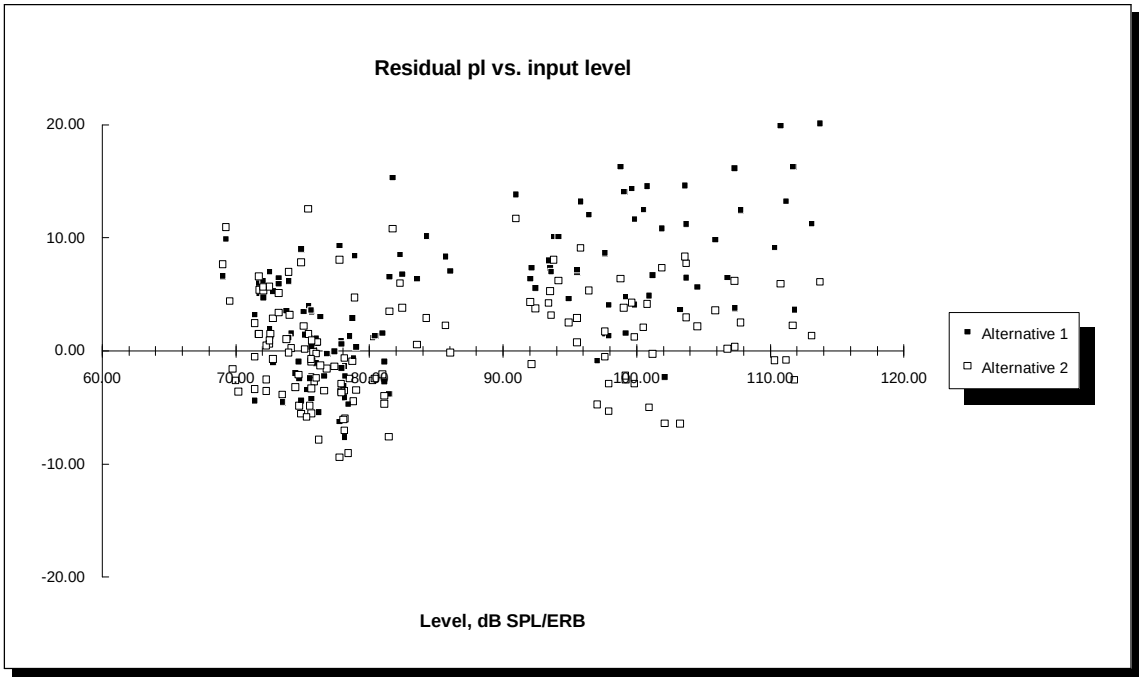

10. *Residual (actual - predicted) low-frequency filter slope parameter, p_l, plotted as a function of masker level in one auditory filter, where the ERB has been broadened by hearing loss. Residuals are shown for two alternatives, 1) threshold and level in addition, and 2) no level effect for thresholds > 20 dB SPL.*

It is clear from Figure 10, that Alternative 2 fits the data better, with residuals spread roughly symmetrically around the abscissa. Furthermore, the residuals of p_l vs. hearing loss (not depicted) are more evenly spread.

As described in Moore and Glasberg (1987), the filter slopes are adjusted according to the summed energy in each E-band. With the combined loss and level effect, the ERB is widened due to hearing loss, thus containing more energy. Consequently, the filter slopes (p_l, p_u) are reduced, and reduced further due to the hearing loss. Effectively, the hearing loss has been included twice in the model. However, with Alternative 2, this has no effect, since ERB's stay normal up to 31 dB SPL, at which point the level-dependency of the filter slope is no longer present.

3.5 Loudness function.

3.5.1 As a function of level and threshold.

As described in section 3.3, the shape of the normal hearing threshold curve can be explained by a linear term, evident from the parallel parts of the equal loudness contours and a threshold term that causes non-parallel curves at low levels. In the case of hearing loss, the threshold curves will be shifted up vertically (expressed in dB SPL), but the 100 phon curve, for instance, may be unaltered compared to the normal-hearing case. The loudness of a tone will thus rise to the same value, but within a much smaller dynamic range.

One possible explanation for this abnormal loudness growth function (recruitment) for impaired hearing are the broader excitation patterns, where the area of the pattern expresses loudness (Evans, 1975b). This hypothesis was not confirmed by Florentine and Zwicker (1979), who found that both recruitment and abnormal spread of masking had to be added to their loudness summation model to explain experimental loudness data. Other results with loudness matching in unilaterally impaired listeners (Moore et al, 1985) support these findings. The authors present the hypothesis, that loudness is encoded by means of nerve fibers with different thresholds, i.e. low-intensity and high-intensity fibers. An impaired ear should then show recruitment due to loss of low-intensity fibers. Simple experiments with the present auditory model also indicate that broader excitation patterns alone do not account for recruitment. However, the broadening of a fixed number of filters, causing them to overlap, requires some sort of 'normalization', for instance based on the rationale that the excitation at one point on the basilar membrane is picked up by a fixed number of hair-cells (Leijon, 1989) - see section 3.5.2.

A separate loudness growth function incorporating the absolute threshold must thus be formulated. Zwicker and Feldtkeller (1967) have described a model for loudness growth in critical bands, termed specific loudness (N'). The model calculates loudness in each

critical band (1 Bark wide bands) from the excitation pattern. Total loudness, N, is then formed as the integral of specific loudness versus critical-band rate.

$$N = \int_{z=0}^{24\ Bark} N'(z)\,dz \qquad \textbf{(16)}$$

In practical applications, the integral is substituted by a summation across bands. The model is similar to Stevens' power law for high excitation levels, with a correction near the threshold of hearing. The loudness growth function depends on the threshold in quiet, which is interpreted as an internal noise source. The specific loudness equation for 1 kHz is presented by Zwicker & Fastl (1990), but the more general formulation of it comes from Zwicker & Feldtkeller (1967). Here, a frequency-dependent detection term is included, s, which is the ratio between the intensity of a just-audible test-tone and the intensity of the internal noise appearing within one critical band around the test-tone.

$$N' = N'_0 \left(\frac{E_{TQ}}{sE_0}\right)^{0.23} \left[\left((1-s) + \frac{sE}{E_{TQ}}\right)^{0.23} - 1 \right] \qquad \textbf{(17)}$$

Here, N'_0 is a scaling constant, s is a detection factor, E is the excitation in the channel caused by the input signal, E_{TQ} is the excitation at threshold, and E_0 is the excitation for 0 dB SPL.

The constant N'_0, is adjusted to meet the boundary condition, that 40 dB SPL at 1 kHz should produce 1 sone as total loudness. At 1 kHz and for a fixed s = 0.5 (moved out from the first set of brackets), the value should be 0.08 (Zwicker & Fastl, 1990) in conjunction with a critical band scale, whereas the value 0.084 has been suggested by Moore & Glasberg (1986) when an ERB-scale filterbank is employed.

The factor s indicates the signal-to-noise ratio required to detect the tone. By letting s vary with frequency (Zwicker & Feldtkeller, 1967), the model is generalized to other frequencies. This factor ("Schwellenfaktor" - Zwicker & Feldtkeller (1967), Bild 39,4) is shown graphically and can be approximated as a piecewise linear function in a coordinate

system with dB and logarithmic frequency axes. This expression is converted from dB by taking the antilog, and we thus get:

$$s = 10^{(-2-2.2\log(\max(f/0.32,1)))/10} \quad \textbf{(18)}$$

where f is the frequency in kHz. With an adjustable s, this must be included in the first bracket term of eqn. (17), and N_0' is instead set to 0.068 (Zwicker & Feldtkeller, 1967).

In the specific loudness equation (17), E_{TQ} is the excitation at threshold in quiet, which can also be interpreted as internal masking noise, and E_0 is the excitation that corresponds to 0 dB SPL. These variables need to be set in the model, in order to calculate specific loudness. In the current implementation, these two quantities are calculated by passing a complex of pure tones, with one tone centered in each band. To set E_0, a 0 dB SPL pure tone is used in each channel and to set E_{TQ}, the tones are set at the hearing threshold level (dB SPL, interpolated in a dB - E coordinate system identical to the perceptual frequency scale of the model). This approach has limitations, since it simulates simultaneous presentation of several pure tones, instead of separate presentation as in a hearing test. The advantage of avoiding the band interaction is, that initialization is relatively fast. For high threshold levels, there may be a considerable widening of the model filters, thus obtaining a very high threshold excitation. The resulting loudness growth curve have elevated thresholds compared to the actual thresholds. Therefore, the widening of the filters with hearing loss is disabled during initialization, and the resulting loudness growth curves are properly aligned with the thresholds. For subjects with very poor frequency selectivity, this approach may be incorrect.

Since specific loudness is a power function, it should approach a straight line in a log-log coordinate system. This is shown in Figure 11, for 6 levels of threshold excitation, 0 - 50 dB in 10dB steps. The asymptote for high excitation levels is a power law with exponent 0.23. The loudness growth model was originally based on stationary sounds, but it is

applicable to fluctuating signals as well (Zwicker & Terhardt, 1979) as in the present model.

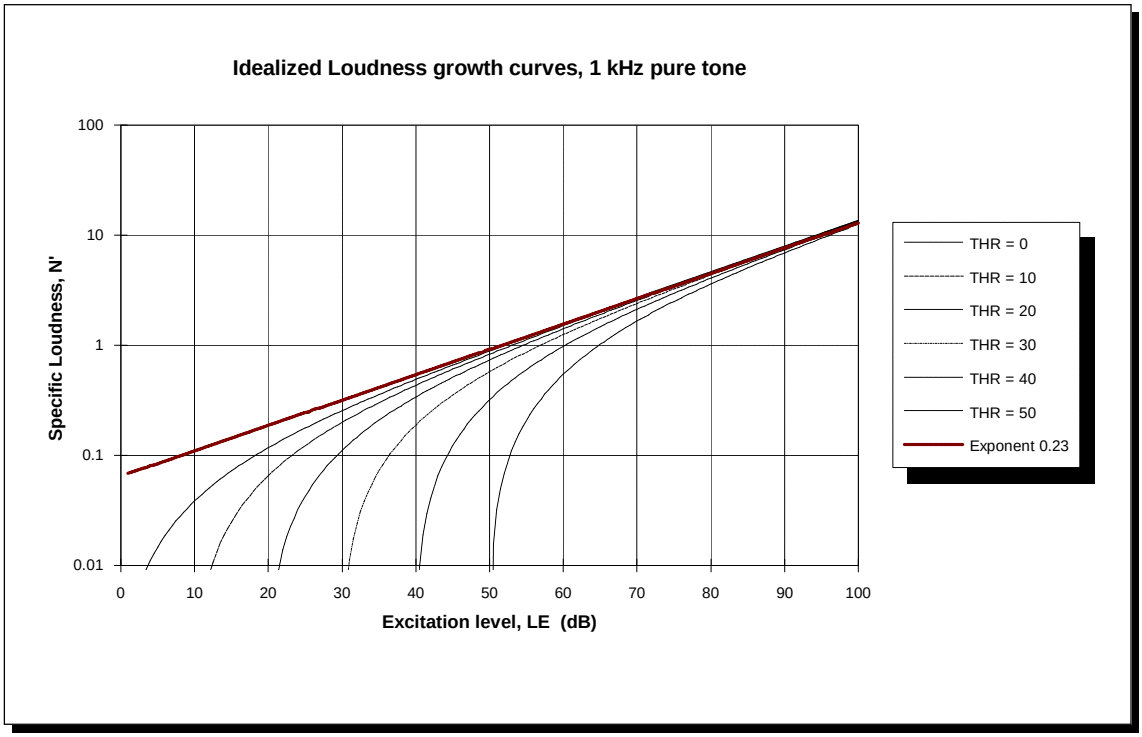

11. *Theoretical growth of specific loudness for various thresholds as a function of excitation, E in the auditory filter channel. Also shown is the asymptotic line* $(E/E_{0})^{0.23}$.

If a cochlear hearing loss can be simulated by normal hearing plus masking noise, the above should represent impaired hearing as well. The current model thus appears reasonable, and the loudness growth curve is qualitatively correct (Scharf, 1978a). Other data available are individual equal loudness contours for hearing-impaired subjects with sloping high-frequency losses from Lippman et al (1981) and Barfod (1976). The loudness growth function for abnormal thresholds can be derived from these data under the assumption that loudness growth is normal at low frequencies. However, these data are all for individual subjects and are thus difficult to use for a general model.

Group results for the loudness growth function in hearing-impaired listeners have been provided by Hellman and Meiselman (1990). Loudness growth functions were obtained for 100 hearing-impaired listeners (primarily bilateral, noise-induced losses) by means of absolute magnitude estimation (assigning a number to the perceived loudness), absolute

magnitude production (adjusting the level of a tone to match an assigned number) and cross-modality matching (adjusting the level of a tone to match the perceived length of a line on a screen). These data were well fitted by a power function (Zwislocki, 1965), that subtracts the loudness of the internal masking noise (equivalent power of the threshold raised by the exponent 0.27) from the loudness of the summed power of tone and internal masking noise. This model is qualitatively identical to equation 17, which can be seen by rearranging the terms in equation 17.

The theoretical models presented here are based on a binaural listening situation, and must be modified for the monaural situation. At high levels, the binaural loudness corresponds to an increase in monaural signal level by 10 dB, corresponding to a doubling of loudness (Humes & Jesteadt, 1991). This simply implies that binaural loudness is a simple addition of the loudness from each ear. Other results indicate that loudness is increased by a factor between 1.7 and 2 (Scharf & Houtsma, 1986). The current model uses a simple summation, but assumes two completely identical ears. The asymmetrical case is not included in the model. Close to threshold, where detection is the main effect rather than loudness rating, the loudness growth curve is much steeper. The binaural detection threshold is improved by 3 dB (i.e. half power) as in two power detectors with correlated input signals and uncorrelated background noise. This corresponds to a doubling in loudness on the steep section of the curve (Scharf & Buus, 1986). Equation 16 can then be modified to monaural loudness by halving the loudness and using the monaural threshold excitation, ETQM:

$$\hat{N} = \frac{\hat{N_0}}{2}\left(\frac{E_{TQM}}{sE_0}\right)^{0.23}\left[\left((1-s)+\frac{sE}{E_{TQM}}\right)^{0.23}-1\right] \qquad \textbf{(19)}$$

In the binaural case, we then use the binaural threshold excitation instead:

$$E_{TQ} = \frac{1}{2}E_{TQM} \qquad \textbf{(20)}$$

Loudness near the uncomfortable level (UCL) is an important aspect of the model, since loudness discomfort and output limiting are common and critical issues in hearing aid fitting. Assuming that pure-tone UCL data is available for a subject, the model could

also somehow encode UCL, either as a separate output or as a different loudness value. A proposed encoding of UCL is presented in Appendix 8.2, with the loudness value rising steeply near UCL. This encoding has not been evaluated further.

For high sound levels, the acoustic reflex in the middle ear introduces a frequency-dependent attenuation of the incoming sounds, primarily for low frequencies. This will modify the input spectrum and thus the level-dependent masking effects and decrease loudness. The current model does not include acoustic reflex.

3.5.2 Loudness summation in hearing-impaired listeners.

The model structure originates from the normal ear, with 33 channels representing the 33 auditory filters that are present when listening to broad-band sounds. In the impaired ear, the broadened filters are fewer with larger spacing along the basilar membrane. In a fixed channel model, the broadening of the auditory filters causes them to overlap, and the same energy or 'excitation' is included more than once in the summed loudness. A physiological interpretation is that the excitation at one point on the basilar membrane is picked up by a fixed (but reduced due to hearing loss) number of hair-cells (Leijon, 1989).

In Zwicker's loudness model, the total loudness is formed by an integration of specific loudness along the critical-band rate (Bark) scale (eqn. 16), which in a fixed channel model can be approximated by a sum of the specific loudness contributions from each filter channel:

$$N = \sum_{i=0}^{24\ \mathrm{Bark}} \hat{N}(i) \qquad \textbf{(21)}$$

Leijon (1989) modifies the specific loudness by a filter widening factor that is specified for a given subject. To make the loudness model simulate recruitment correctly, i.e. normal loudness at high levels, the power-law exponent is also modified (not constant 0.23).

In the present model, the filter bandwidth increases with hearing loss as given by equation 12, which can be used to compensate the loudness summation. Modifying to an ERB-rate scale, we get:

$$N = \sum_{i=0}^{N_{ERB}} \hat{N}(i) \frac{ERB_{NH}}{ERB_{HI}} = \sum_{i=0}^{N_{ERB}} \hat{N}(i) \frac{-0.29+0.014\&30.7}{-0.29+0.014\max(30.7, THR)} \quad \textbf{(22)}$$

This formulation preserves the original properties of the Zwicker & Fastl model. If this is not sufficient, the next step would be to modify the power-law exponent. The loudness growth function for normal and impaired hearing is evaluated in 4.3.1.

3.6 Temporal processing.

The current model is power-spectrum based and no attempt has been made to model temporal processing, such as temporal integration or forward and backward masking. The spectrally-based model will most likely disregard much of the fine-grain temporal structure of speech, considered important for speech recognition. For estimation of sound quality, however, spectral information may be adequate. Temporal processing was thus considered a secondary factor, and within the time limits of the project, it was not possible to implement and verify temporal factors in the auditory model.

4 Verification.

4.1 Test design and stimuli.

The auditory model has been tested using a number of test stimuli (signals). All synthetic signals were generated using the HyperSignal Workstation signal processing package and stored in its .TIM time series format. Shaped noise was made from white noise by convolving with a filter designed with the FILTSPEC program (ODIN, 1988). The convolution was done using the CONVOL program (Nielsen, 1992).

Each model test session uses the AUDMOD.EXE program with a unique parameter text file in the special file format required (see appendix 8.1 for an example and explanation).

4.2 Frequency selectivity.

The frequency selectivity in the literature is often characterized as either masking patterns for narrow- or broadband stimuli, which are roughly equivalent of excitation patterns. The difference between excitation and masking pattern depends on the detection threshold of the probe signal in the masker within a given critical band. Typically, the power of the pure tone is a few dB below the power of the masking noise in one critical band. This is equivalent of the factor s (section 3.5.1 and Zwicker & Fastl, 1990), which varies with frequency, or the constant K factor deduced by Pavlovic (1987) from Zwicker's data.

4.2.1 Excitation patterns, pure tones.

To illustrate the model behavior, the excitation patterns have been plotted for two pure tones at increasing input levels. The excitation pattern is the output of the model across channels. The physiological equivalent of this is the basilar membrane vibration pattern along the place dimension. Examples of excitation patterns for 0.5 and 4 kHz pure tones are shown in Figure 12, along with the quiet (threshold) excitation. The area between the pure tone excitation pattern and the threshold excitation determines the loudness of

the stimulus. It is clear from the figure, that the tails of the 4 kHz patterns are missing, thus leading to a low estimate of loudness, in particular at high levels, where a large area is missing. This problem can be alleviated by using the model with a higher input sampling rate and a higher upper frequency limit.

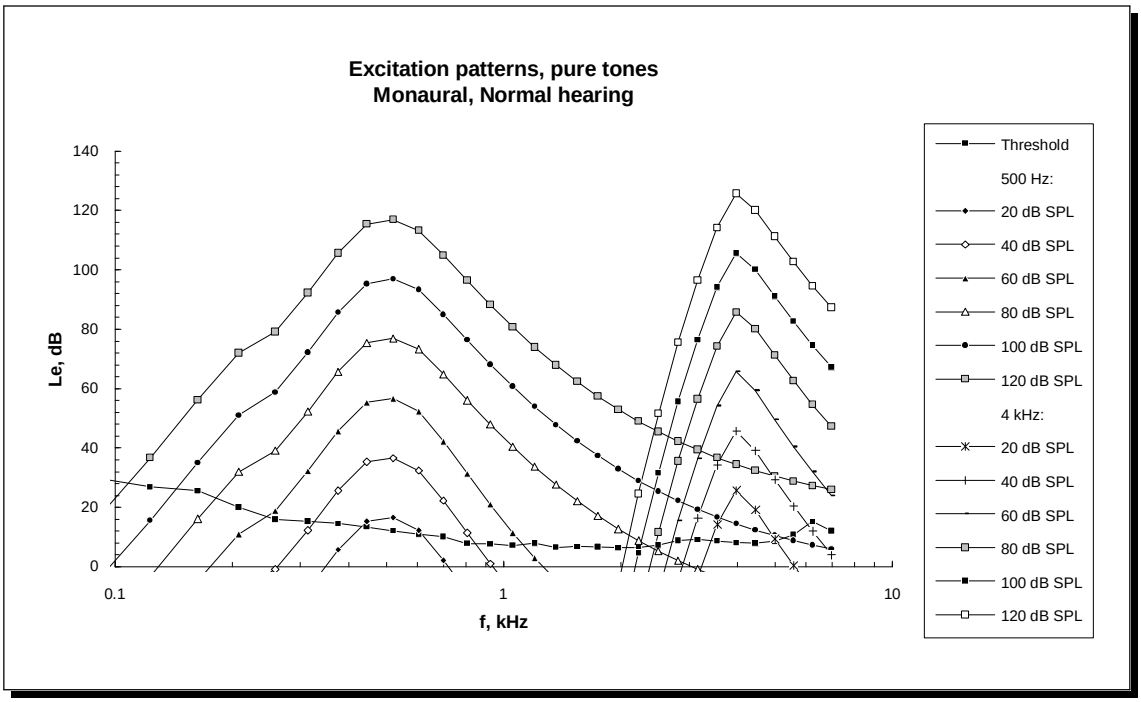

12. *Pure tone excitation patterns for 0.5 and 4 kHz pure tones at various levels compared to the threshold excitation. The tails of the 4 kHz patterns are missing due to the upper frequency limit in the model at 7 kHz.*

For a 1 kHz pure tone at various levels, masking patterns have been presented by Zwicker and Fastl (1990). These experimental pure tone masking patterns are irregular close to the masker frequency and multiples of it, due to detectable beats between the masker and the probe tone. These beats are detected by the subject, and the normal masked threshold becomes difficult to obtain. The auditory model does not account for beats, due to its power-spectrum foundation. Thus, it seems reasonable rather to compare the model pure-tone excitation patterns with masked thresholds for a narrow-band noise signal. The noise signal has a bandwidth less than one critical band (< 1 Bark), to excite only one auditory filter. This comparison of model excitation patterns with narrow-band noise patterns is shown in Figure 13. The masked thresholds were

read off a graph (Zwicker & Fastl, 1990, Fig. 4.4) and entered in a spreadsheet, resulting in not perfectly smooth curves.

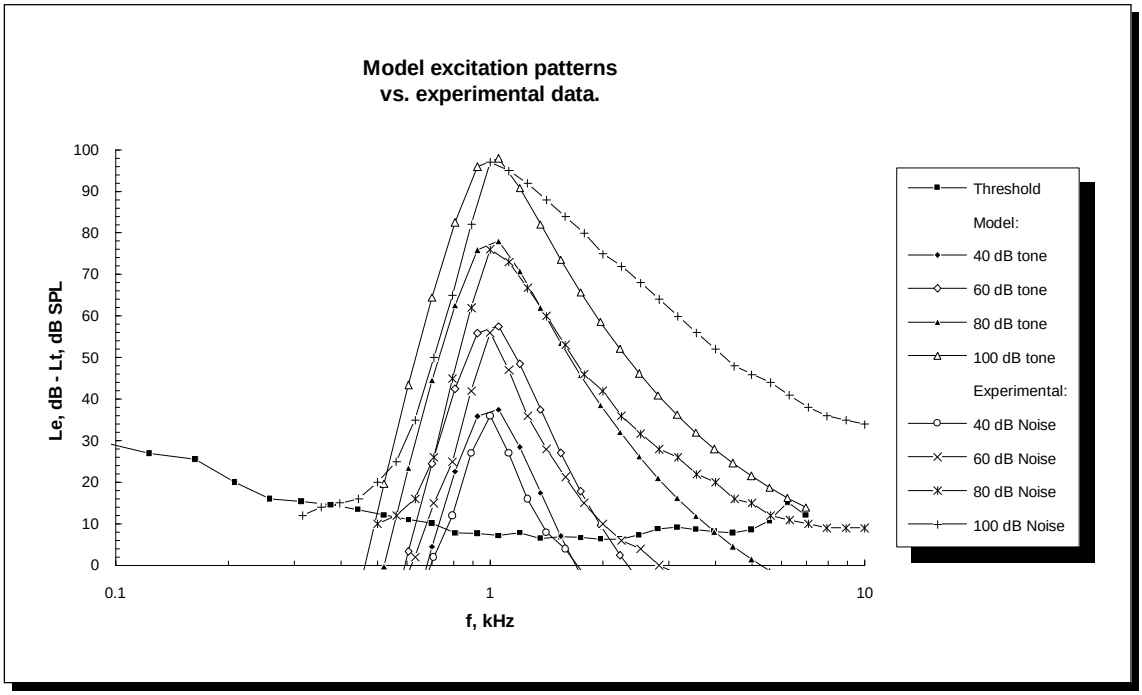

13. *A comparison of model excitation patterns for pure tones and masked thresholds for critical-bandwide noise (Zwicker & Fastl, 1990, Fig 4.4). L_e is the internal model excitation, and L_t is the level of the just-detectable test tone.*

For low signal levels, the model curve coincides well with the masked thresholds. At most levels (60-80-100 dB SPL), the model output extend further below the masker frequency than the masked thresholds patterns. Thus, the two sets of experimental thresholds are not identical, despite both being within the limits of one critical band. At high levels (80-100 dB SPL), the masked threshold patterns have more shallow slopes than the auditory model. This may be due to the upper limit for increasing filter bandwidth in the model, at 71 dB SPL/ERB (see Figure 10), apparent from the parallel curves at 80 and 100 dB SPL. An increase of this limit could be considered, however this would also require an increase of the upper limit for hearing loss with enhanced tuning at low levels (Figure 9).

4.2.2 Noise signals.

For a white noise masking signal, the classical masked pure tone threshold (Zwicker & Fastl, 1990, Fig. 4.1) follows a horizontal line up to approximately 500 Hz, followed by a sloping line at +10 dB per decade (+3 dB/octave).

For white noise at varying levels, the auditory model excitation patterns are shown in figure 14. Also shown is the masked threshold for a white noise signal at 30 dB SPL/Hz, approximated by a two-segment line (from Zwicker & Fastl (1990), fig. 4.1).

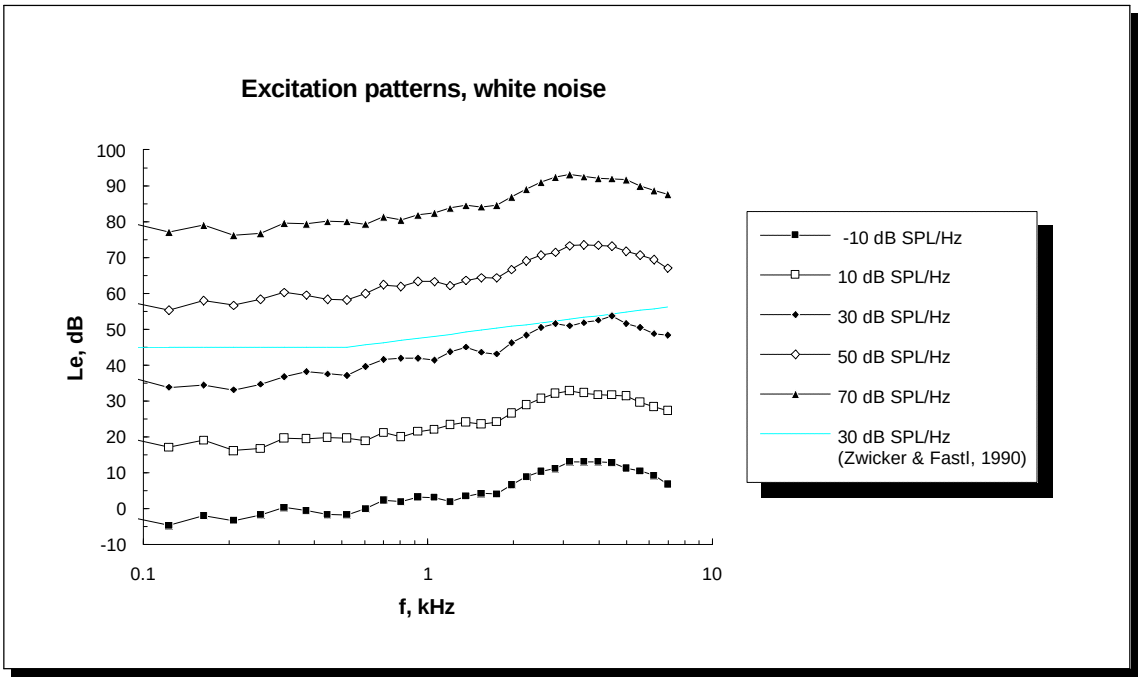

14. *Excitation patterns for a white noise signal at various levels, compared to an idealized model of masked threshold for a 30 dB SPL/Hz white noise signal.*

There is a considerable difference between the model output and the masked thresholds, at low frequencies (~ -10 dB). The bandwidth of the ERB-filters continues to decrease below 500 Hz, whereas the classical critical-band scale has constant bandwidth (= 100 Hz) below 500 Hz (Moore & Glasberg, 1987). Therefore, the excitation pattern continues to drop below this frequency. The model output curve is also irregular compared to the masking curves from Zwicker & Fastl (1990) - probably due to a smoothing of their data.

Another relevant noise signal in psychoacoustic testing is the so-called uniform exciting noise (UEN), ie. noise that causes the same excitation in all channels. The spectrum of such a signal has been proposed by Zwicker & Feldtkeller (1967). Their noise signal was tested in the auditory model along with a white noise signal (see Figure 15). The purpose of UEN is to measure psychoacoustic parameters, without misleading results due to the spread of excitation, for instance to measure the loudness growth function in one auditory filter channel (specific loudness - see section 3.5.1).

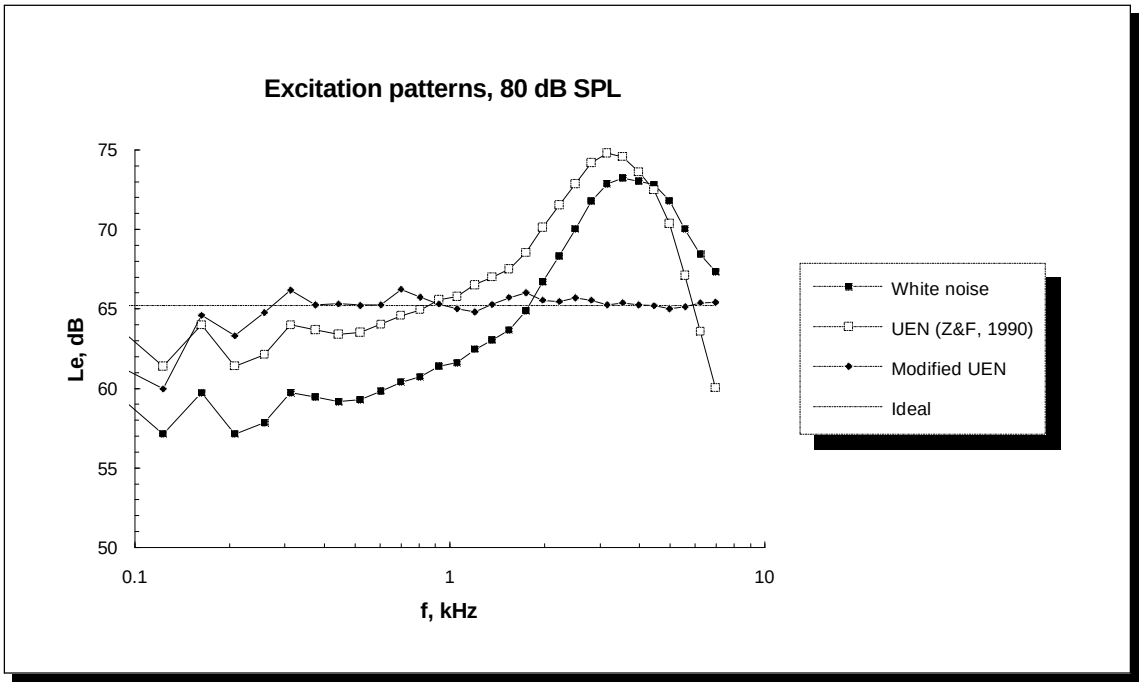

15. *Excitation patterns for white noise, uniform exciting noise (Zwicker & Fastl, 1990) and modified uniform exciting noise, all at 80 dB SPL. Also shown is the ideal excitation, when the signal power is evenly distributed across channels.*

The original UEN does not account for the ear-canal response around 3 kHz, as seen from the excitation pattern.

For the purpose of further testing of the specific loudness growth function (section 4.3.1, Figure 21), a modified UEN was then created as follows: The excitation pattern for a 80 dB SPL white noise signal (40 dB SPL/Hz) was obtained, and a 256-tap digital filter with the inverse amplitude response was then designed by means of the FILTSPEC program (ODIN, 1988). By convolving the white noise signal with the digital filter, the modified UEN was obtained. At low frequencies (< 300 Hz), the FFT-analysis framesize

in the auditory model and the length of the digital filter were both too short to control and measure the frequency response properly, as seen in the graph.

4.2.3 Impaired frequency selectivity.

Frequency selectivity in hearing impaired listeners has been the subject of several studies - Florentine et al (1980), Ludvigsen (1985) and Dubno & Schafer (1992), to name a few. For comparison with the auditory model, the recent results of Dubno & Schafer (1992) have been chosen, due to a straightforward stimulus choice and results that were easily obtained from the graphs in the paper. The subjects were six individuals with mild-to-moderate sensorineural hearing losses, four with typical sloping, high-frequency losses and two with flat hearing loss. Masked pure-tone thresholds were obtained with narrow-band 200 Hz noise bands, centered at 1200 Hz. The test-tone frequencies were 0.63, 0.80, 1.00, 1.20, 1.25, 1.40, 1.60, 2.00, 2.50, 3.15, and 4.00 kHz, and all signals were presented via a TDH-49 headphone. All threshold values are provided in dB SPL, presumably recorded on a 6 cm^3 (IEC303) coupler.

For the model simulations, the four subjects with sloping losses were averaged to one group, ie. absolute thresholds were averaged and masked thresholds were averaged. Same procedure was used for the two subjects with flat losses. The 200 Hz NB-noise signals in the experiment was slightly wider than a normal critical band centered at 1200 Hz (190 Hz, Zwicker & Fastl (1990)) and wider than one ERB-band (155 Hz, Glasberg & Moore (1990)). It was presented at two spectrum levels, 40 dB SPL/Hz and 60 dB SPL/Hz. For the present auditory modeling, a 1200 Hz pure-tone signal with the same sound pressure level was used for simplicity (63 dB SPL and 83 dB SPL), which can be justified because of the absence of beats (difference tones) in the model.

The results for the 40 dB SPL/Hz masker are shown, only for the sloping loss group, in Figure 16.

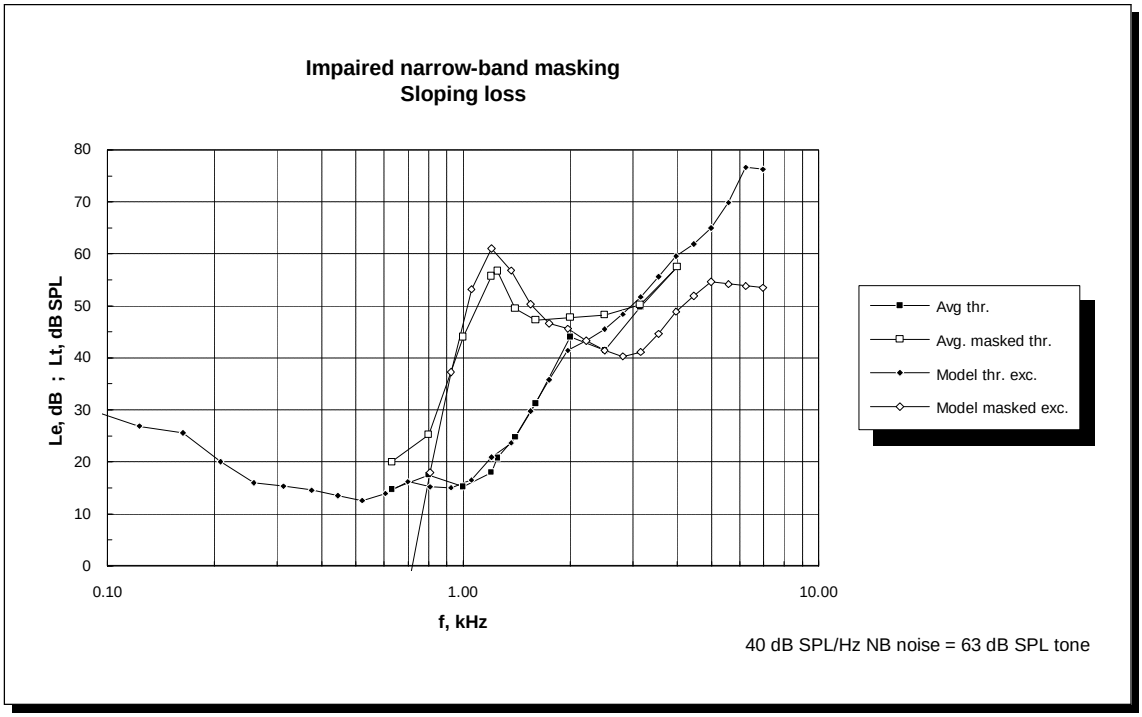

16. *Average masked and absolute thresholds for four subjects with sloping loss (Lt, in dB SPL), compared to the excitation in the auditory model (Le, dB). The masker was a 1200 Hz, 200 Hz-wide noise band at 40 dB SPL/Hz, and the model stimulus was a 1200 Hz pure tone at 63 dB SPL.*

The model excitation pattern for the threshold matches the absolute thresholds in the range were they were obtained (630 Hz - 4 kHz). Outside this range, thresholds were extrapolated to normal hearing at low frequency and increasing loss at high frequencies. The close match was expected, since the model parameter file contained the audiometric thresholds, expressed in dB HL.

In the masked situation, there is a good agreement between the experimental data and the model output. The upward spread of masking is reproduced by the model, with some deviation close to the absolute threshold. The model excitation pattern does not approach the absolute threshold asymptotically, but simply intersects it. This deviation could be alleviated if the threshold parameter, *r*, was included in the *roex* filter shape (equation 2, section 3.4), instead of using threshold in the loudness function only.

For the 60 dB SPL/Hz masker and the sloping loss group, the results are shown in Figure 17.

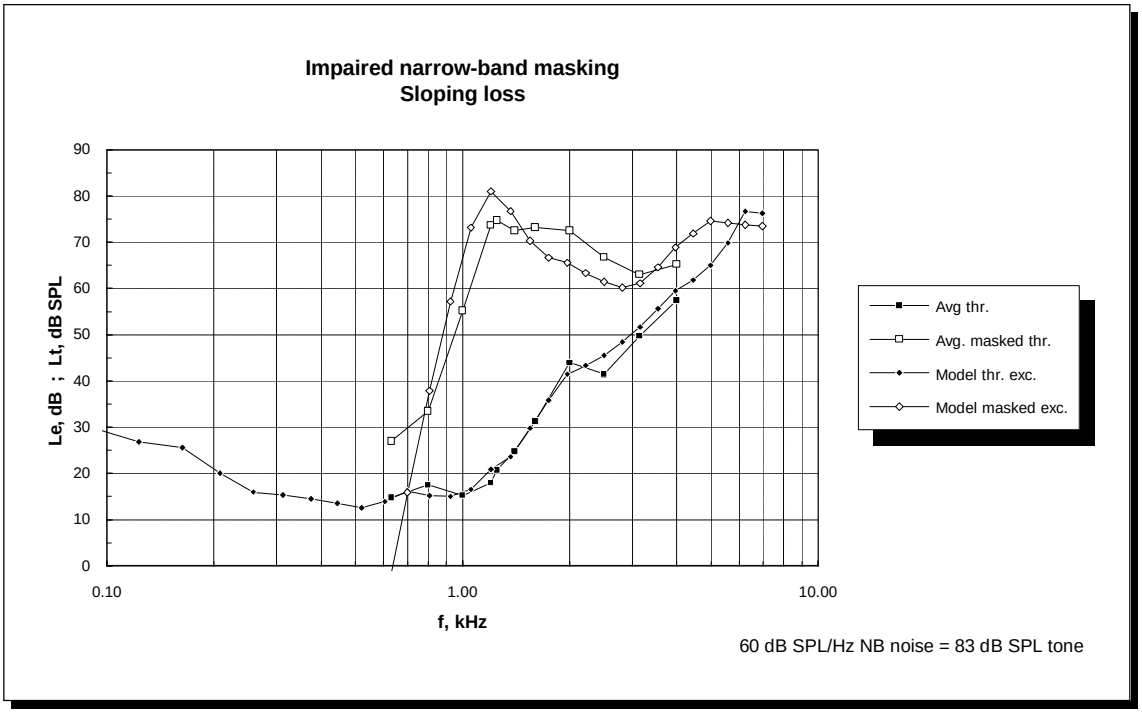

17. *Average masked and absolute thresholds for four subjects with sloping loss (Lt, in dB SPL), compared to the excitation in the auditory model (Le, dB). The masker was a 1200 Hz, 200 Hz-wide noise band at 60 dB SPL/Hz, and the model stimulus was a 1200 Hz pure tone at 83 dB SPL.*

The masked thresholds indicate a larger amount of upward spread of masking than the model, but there is a reasonable agreement. The model excitation pattern bends upward again above 3 kHz and runs parallel to the threshold excitation, due to almost complete loss of frequency selectivity for the large losses present at higher frequencies. Thus, the high-frequency filters are able to "see" the stimulus at 1200 Hz. This high-frequency excitation may be overestimated, but no firm conclusion can be made, since the hearing losses above 4 kHz were extrapolated for the simulations.

The same overestimated upward spread of masking is evident for the two subjects with moderate, flat losses as shown in figure 18.

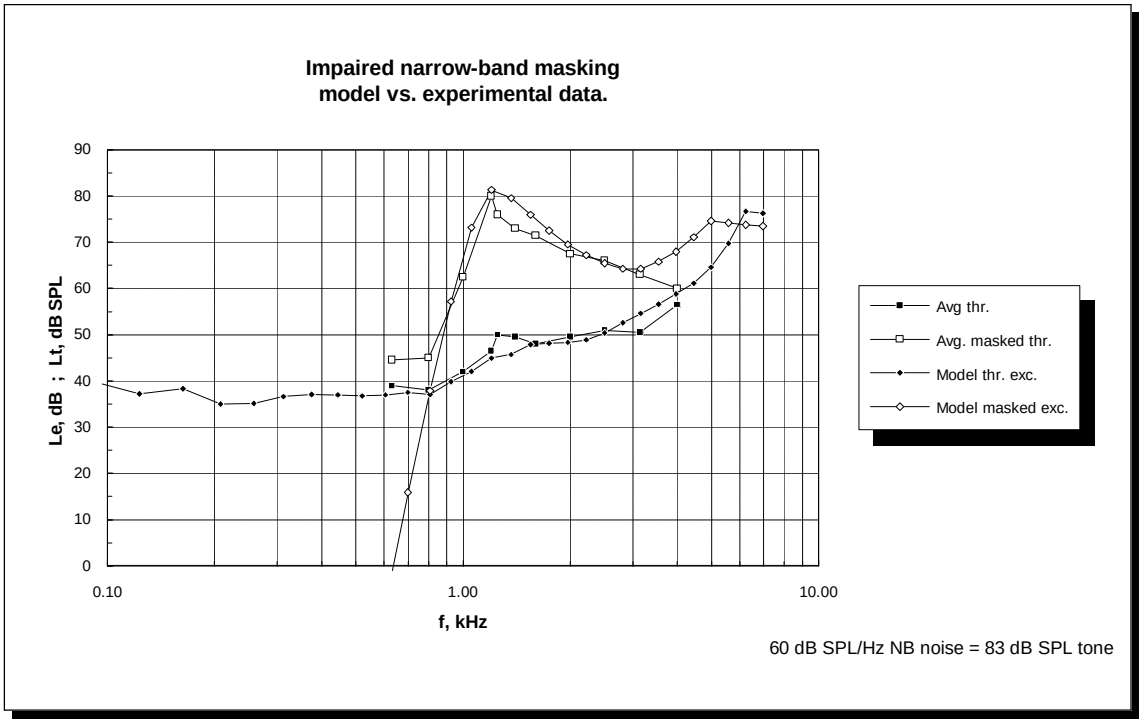

18. *Average masked and absolute thresholds for two subjects with flat loss (Lt, in dB SPL), compared to the excitation in the auditory model (Le, dB). The masker was a 1200 Hz, 200 Hz-wide noise band at 60 dB SPL/Hz, and the model stimulus was a 1200 Hz pure tone at 83 dB SPL.*

Except for this discrepancy and an elevated masked threshold at 630 Hz relative to the model, there is good agreement between the two curves.

Based on these three cases, the model appears to represent the reduced frequency selectivity in mildly-to-moderately hearing-impaired listeners well on the average. There may be large individual differences (Tyler, 1986), that a general model cannot represent, unless frequency selectivity is measured on an individual basis.

4.3 Loudness.

4.3.1 Loudness growth in normal and impaired hearing.

The loudness function in the model was first compared to loudness growth functions for normal hearing. The stimulus used for this was pure tones at octave frequencies. The signal files contained 26 frames, with a stepwise increase of 2 dB between frames, thus

covering a 50 dB dynamic range. If necessary, two overlapping 50 dB ranges were used (by changing the auditory model parameter file), to cover the entire dynamic range.

Data on binaural loudness in sones was obtained from Scharf (1978b). For 1 kHz, the loudness as function of dB SPL is listed in a table, whereas the loudness growth functions for other frequencies are derived from the ISO 226 (1987) equal loudness contours, that originate from Robinson and Dadson (1956).

The loudness growth functions for the auditory model are shown in Figure 19 along with the 1 kHz loudness growth function from Scharf (1978b).

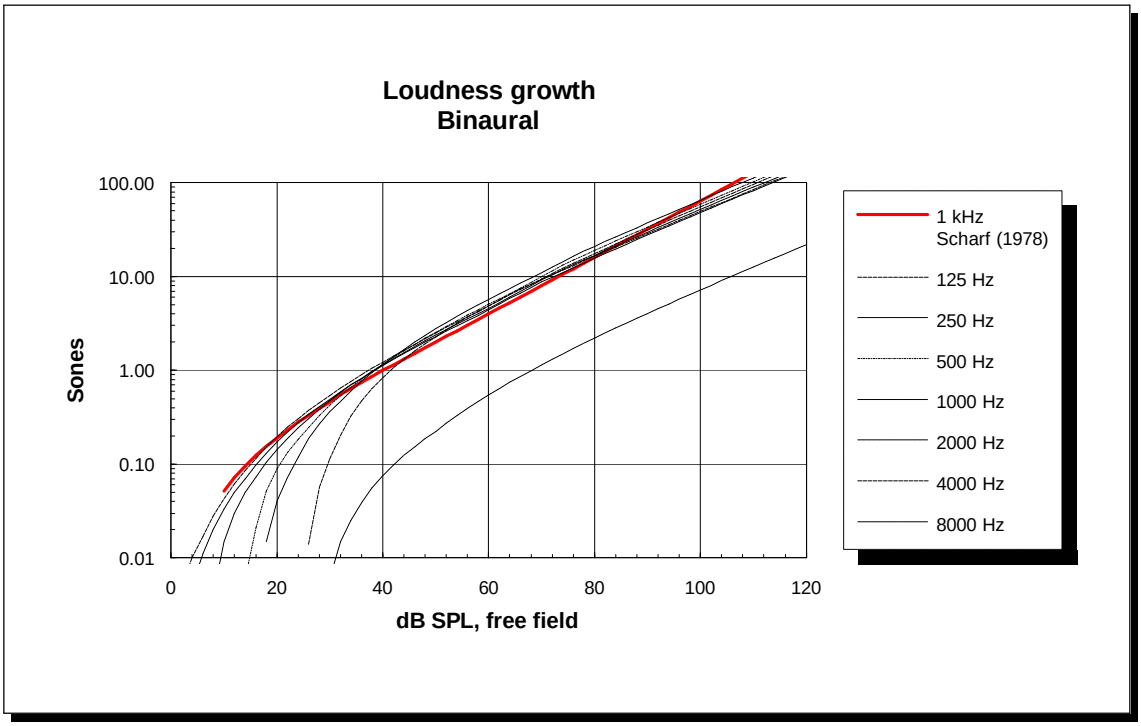

19. *Binaural loudness growth functions for various frequencies. The 1 kHz loudness function can be compared to actual loudness data from Scharf (1978b).*

The actual loudness curve from Scharf follows the power law above 40 dB SPL:

$$N = k\left(\frac{P}{P_0}\right)^{0.6} = k\left(\frac{I}{I_0}\right)^{0.3} \qquad \textbf{(23)}$$

which is a straight line in a dB - log sones plot. k is chosen to obtain 1 son at 40 dB SPL. According to Scharf (1978b), all the loudness curves should coincide with this line

at high levels, except the 8 kHz curve, which is shifted down, due to a larger transmission factor (e.g. attenuation) at this frequency. At low frequencies, we see elevated thresholds and thus more rapid growth of loudness near the threshold.

The 1 kHz model curve drops down towards thresholds at a slightly higher level, and the curve is shifted roughly 4 dB at 0.05 sones, an acceptable deviation. At higher levels (40-80 dB SPL), there is a slight overshoot compared to the power law line for all frequencies. Since the model uses a different filter shape and a higher number of critical bands (30 in the range 87 Hz - 7 kHz vs. Zwicker's 21 in the same frequency range), the total loudness may be higher, when no adjustment of N_0' has been made. Without any precise, quantitative description of loudness, there is no obvious reason to make a modification.

At higher levels (~80 dB SPL), the loudness curve drops below the power law line, in particular for the higher frequencies. This is probably due to the upper frequency limit (10 kHz) that was used in the current simulations, which limits the upward spread of masking, cutting off the high-frequency tail of the excitation pattern and resulting in an incorrectly low loudness. These excitation patterns are shown in Figure 12. Future simulations with higher bandwidth (ie. higher sample rate) might confirm this.

When hearing loss is introduced, the model should exhibit 'recruitment', ie. abnormally steep growth of loudness. For a series of flat hearing losses, the 1 kHz loudness growth function was evaluated as shown in figure 20.[2]

[2] The curves were obtained for a 1060 Hz pure tone, since this frequency is centered in a filter channel of the model.

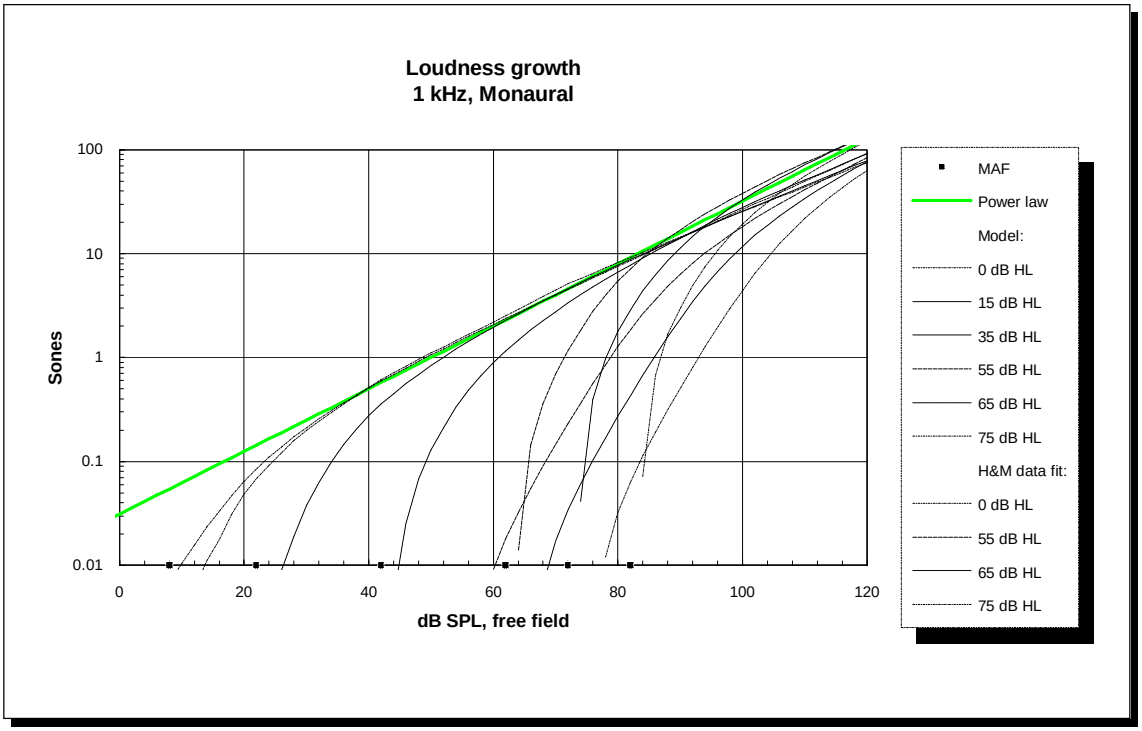

20. *Loudness growth as a function of level and hearing loss. The heavy line represent the 0.3 exponent power law and the markers along the abscissa indicate the monaural free-field threshold. Also shown are the fitted loudness growth functions to experimental data by Hellman and Meiselman (1990).*

In the figure, the free-field thresholds are indicated with filled squares along the abscissa. In a log sones plot, the loudness function should approach these levels asymptotically, since per definition loudness is $N = 0$ at threshold. This is clearly the case for high thresholds, whereas the 0 and 15 dB HL losses have more shallow slopes close to threshold. The recruitment effect is very obvious, since all loudness functions approach the power law line at high levels (> 100 dB SPL). A modification of the loudness growth exponent at high levels as proposed by Leijon and discussed previously (section 3.5), is thus not needed For small threshold values, there is a slight underestimation of loudness for high levels, due to the aforementioned band limiting of upward spread of masking. For high threshold values, there is a slight overestimation, which is due to the increased spread of masking, ie. almost no frequency selectivity.

Hellman & Meiselman (1990) presented data on loudness growth functions for hearing-impaired listeners with noise-induced losses of 55, 65 and 75 dB HL. No detailed statistics on the audiogram shape was presented. The fitted loudness functions

(obtained from the paper) were scaled by means of a spreadsheet program to coincide with the power law at high levels (*1.85) and plotted in Figure 20. Their loudness model for impaired hearing is based on a loudness summation model by Zwislocki (1965). There is a large discrepancy between these data and the model output, ie. the model loudness functions rise more steeply than the fitted lines presented by Hellman & Meiselman (1990). The fitted lines indicate linear growth of loudness near threshold, with the 0.01 sones levels being below threshold, however these lines extend below the lowest loudness value in the actual data (0.4 sones). The large difference between the two models has implications on the degree of recruitment present for a given hearing loss. The Zwislocki loudness model should be subject to more investigation and possibly be implemented in the model in the future.

The correct shape of the specific loudness function is tested by using 'uniform exciting noise' (Zwicker & Fastl, 1990), ie. a noise signal, shaped such that the resulting excitation pattern is flat. The reason for this is that a for a flat excitation pattern, an upward spread of masking will have little or no effect, since there is energy present in all bands. The preparation of such a signal was presented in section 4.2.2. The noise signal was multiplied by a 2 dB step staircase, such that the signal level increased 2 dB per each 8 frames over a 50 dB range. For none or little hearing loss, two overlapping 50 dB ranges were used to cover the entire dynamic range. By averaging 8 power spectra prior to the loudness calculation the result was fairly stable. The obtained loudness curves are still not perfectly smooth as shown in figure 21. The hearing losses simulated in the model were flat, e.g. constant dB HL across the audiometric frequencies.

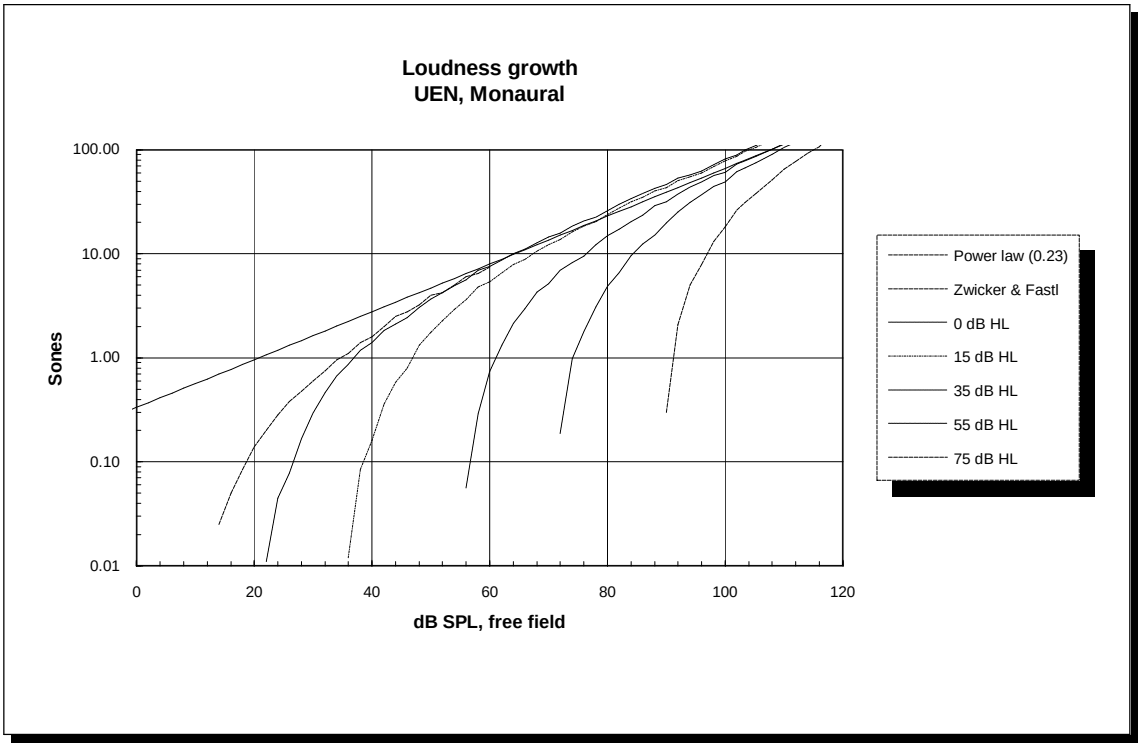

21. *Monaural loudness growth function for uniform exciting noise with various flat hearing losses. Also shown are the power law line for the specific loudness growth function and the measured loudness function near threshold (Zwicker & Fastl, 1990) .*

The model loudness curves were compared to results from Zwicker and Fastl (1990). Their original data on binaural loudness were converted to monaural values by halving the loudness, as discussed in section 3.5.1. At high levels, the model output curves agree reasonably well, when there is a small or no hearing loss. The actual threshold of the model for 0 dB hearing loss is elevated by roughly 10 dB in comparison with Zwicker & Fastl's binaural results, with at least 3 dB due to the missing binaural-to-monaural threshold correction. Even when the model thresholds are approximately correct for pure tone stimuli, it is difficult to predict the absolute threshold of the noise signal, since the detection factor (s in eqn. 16) most likely will be different when broad-band noise signals are detected in the presence of the internal background noise. No further changes were made to the model to correct this threshold deviation.

4.3.2 Equal loudness level contours.

Based on the loudness growth curves from section 4.3.1, equal loudness level contours can be constructed, ie. the level of a pure tone at a given frequency at which the level is equally loud as a 1 kHz tone. Thus, the 20 phon curve is the contour curve indicating the level that a pure tone should have to be perceived as loud as a 20 dB SPL, 1 kHz tone. Since the model output is in sones, the sone value corresponding to each 10 phon increase can be found from the 1 kHz loudness growth curve by Scharf (1978b), shown in Figure 19. The equal loudness curves derived in this way from the auditory model output are shown in figure 22.

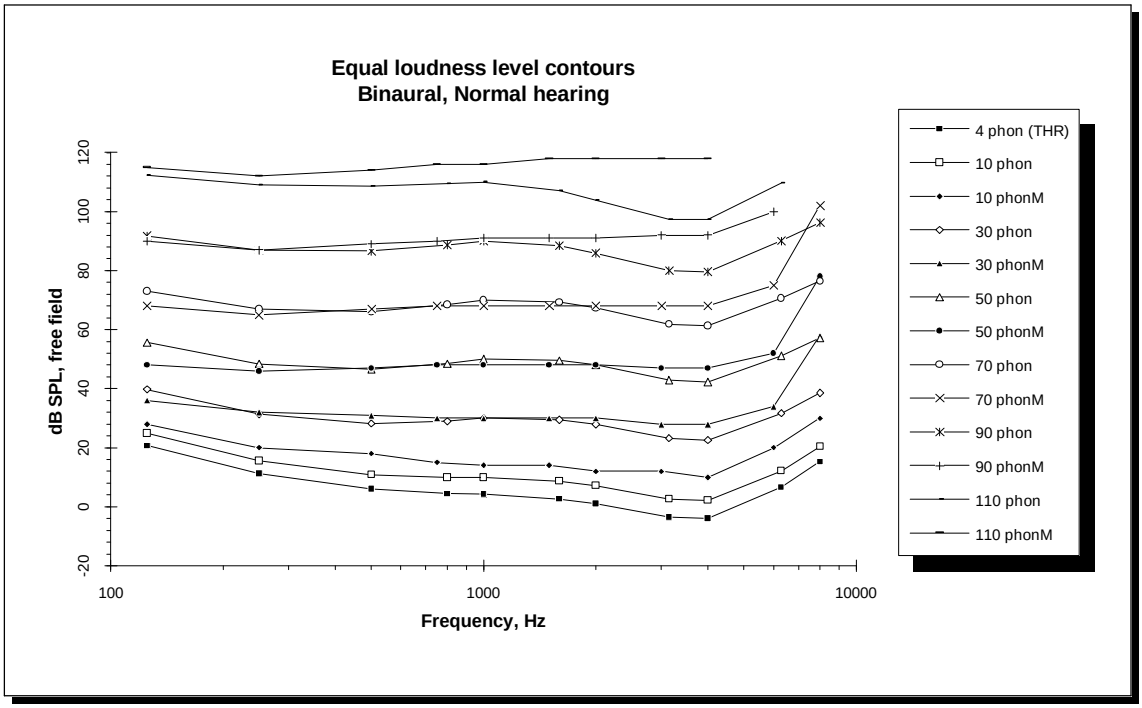

22. *Equal loudness contours derived from model loudness growth functions (indicated as phonM curves) and reference equal loudness curves from ISO226 (indicated as phon curves). The 4 phon curve is the absolute threshold, also termed minimum audible field (MAF).*

The contours derived from the auditory model can be compared to the standard equal loudness level contours published in ISO226. The lowest curve (10 phonM) is elevated, but parallel to the ISO226 curve. This confirms that the effective thresholds in the model are a little to high (figure 20 for 1 kHz). The loudness function initialization procedure used in the model (section 3.5.1) will force the shape of the phon curve to the correct value near threshold. At higher levels (30-50-70 phon), the two sets of curves deviate at

3-4 kHz, ie. the model fails to reproduce the dip in the curves. This could be corrected by using the 100 phon ELC correction curve (flat below 1 kHz) shown in Figure 2, causing the dip to be roughly 5 dB deeper. At higher levels, this difference becomes more pronounced, along with a larger difference at 6 kHz - these differences are equivalent of loudness curves dropping below the power law line as shown in Figure 19. This is due to the upper frequency limit in this configuration of the model that imposes an artificial constraint on the upward spread of masking for high-level, high-frequency signals, as discussed in section 4.2.1. Above threshold, the 8 kHz values are very different, since this frequency is above the highest channel in the present model configuration (7 kHz).

4.4 Temporal resolution.

Since temporal resolution has not been included in the model specifically, the temporal properties have not been evaluated. When the input signal is analyzed in overlapping frames, the model excitation will obviously fade out, as a signal is turned off, thus emulating some kind of post-masking. This will also prevent the model from detecting gaps in the signal, when below a given size. However, a quantification of these properties was not considered meaningful and thus not pursued.

5 Processing of real-world signals.

5.1 Perception of speech sounds.

The obvious advantage of a signal processing structure implemented as a program, as opposed to a mathematical formulation of masking patterns, loudness growth functions etc., is that it can be used to analyze complex patterns and real-world signals. One example of such an application is shown in Figure 23.

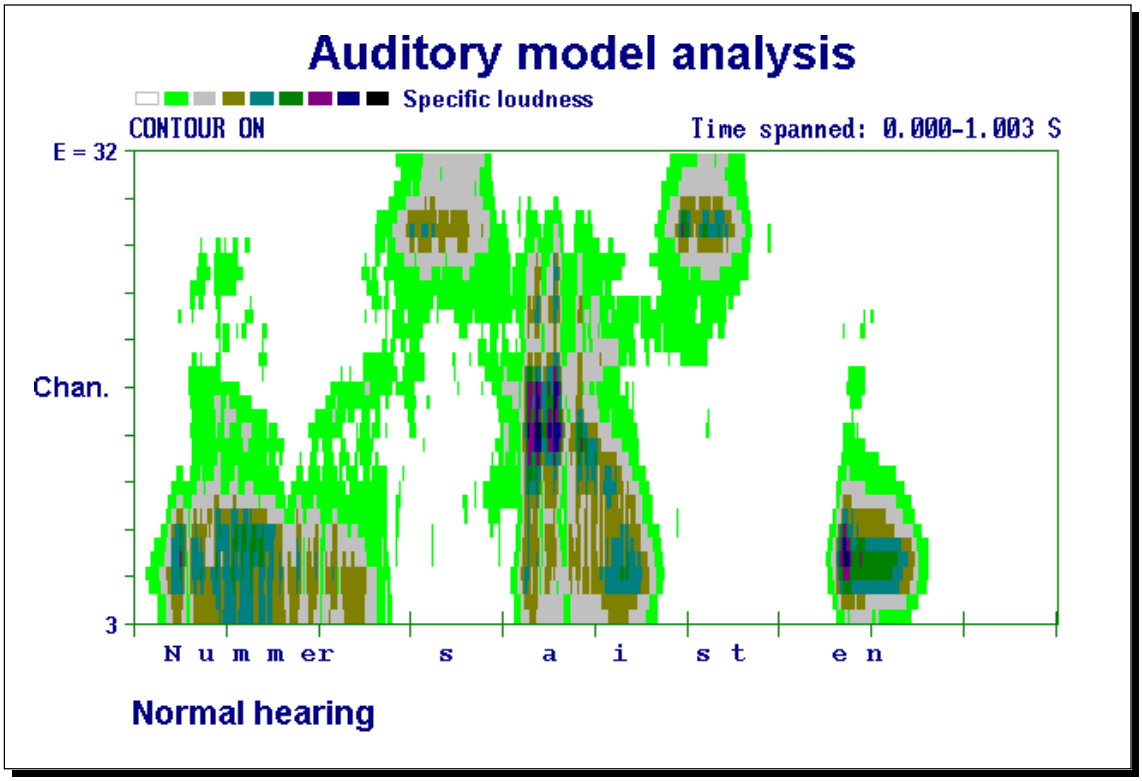

23. *The danish utterance "Nummer saisten" (Number sixteen) processed through the auditory model with normal hearing and viewed as a grey-scale mapping of specific loudness. The signal level was set at 65 dB SPL. The x-axis is time and the y-axis is channel number in the model.*

The 1-second utterance "Nummer saisten" ("Number sixteen") was processed through the auditory model with 33 channels spaced between E = 3 and 32. The signal was processed in 256-point frames with a 75% overlap. The long-term level L_{eq} was set to 65 dB SPL in free field. The grey-scale in the plot is set such that black equals maximum specific loudness and each step represents fixed decrease in specific loudness (ie. a linear scale). Due to the power law used for loudness encoding as opposed to the

log-transformation typically used for excitation patterns, the loudness 'spectrogram' will cover a smaller dynamic range. It is possible to distinguish formant patterns for the vowels, and the general pattern is quite detailed.

The model was then used with a typical sensorineural sloping loss, the average loss from a previous experiment (Nielsen, 1992) was entered. When processing the same utterance without any amplification, the specific loudness 'spectrogram' contains less information as shown in Figure 24.

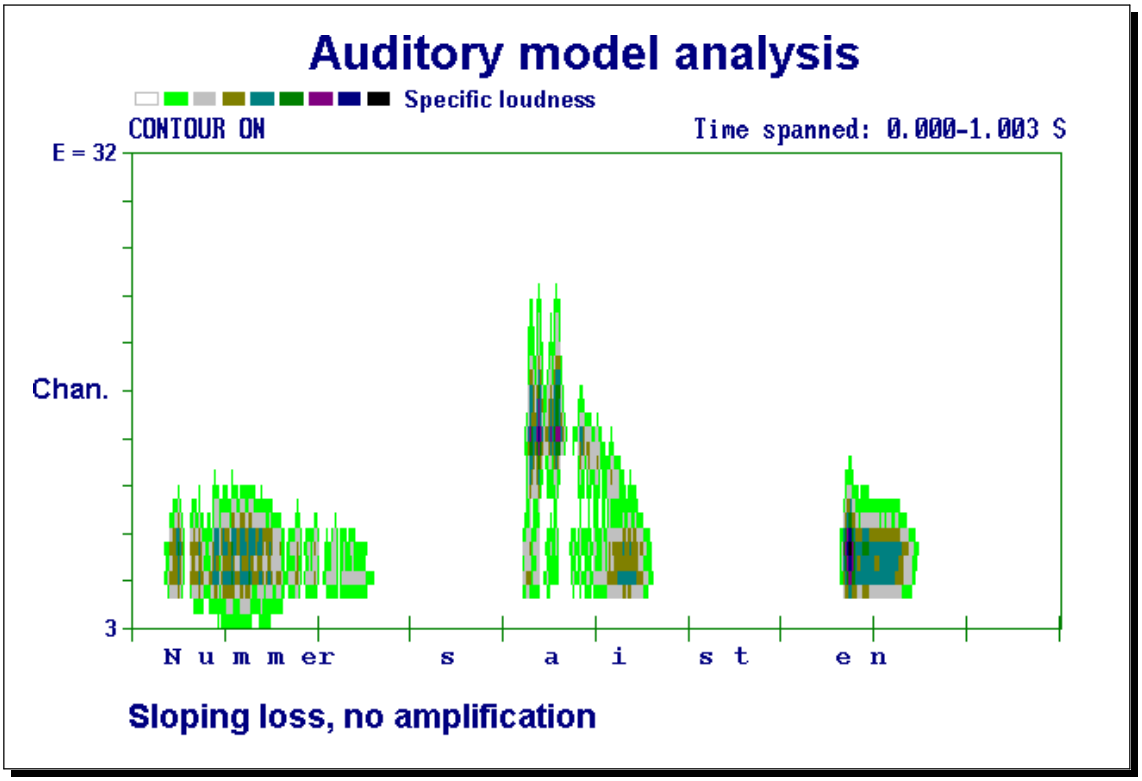

24. *The danish utterance "Nummer saisten" (Number sixteen) processed through the auditory model with a typical sensorineural, sloping hearing loss, and viewed as a grey-scale mapping of specific loudness. The signal level was set at 65 dB SPL, and no amplification was applied. The x-axis is time and the y-axis is channel number in the model.*

Only the low-frequency segments of the signal are visible and the vowel 'a' has less high-frequency information. The next step was to apply a linear amplification to the speech signal, using the POGO II amplification rule (Schwartz et al, 1988) to specify the insertion gain. A 64-tap filter was designed and the signal was convolved with this filter.

The auditory model parameter file used scaling equivalent of an L_{eq} of 65 dB SPL prior to amplification. The result is shown in Figure 25.

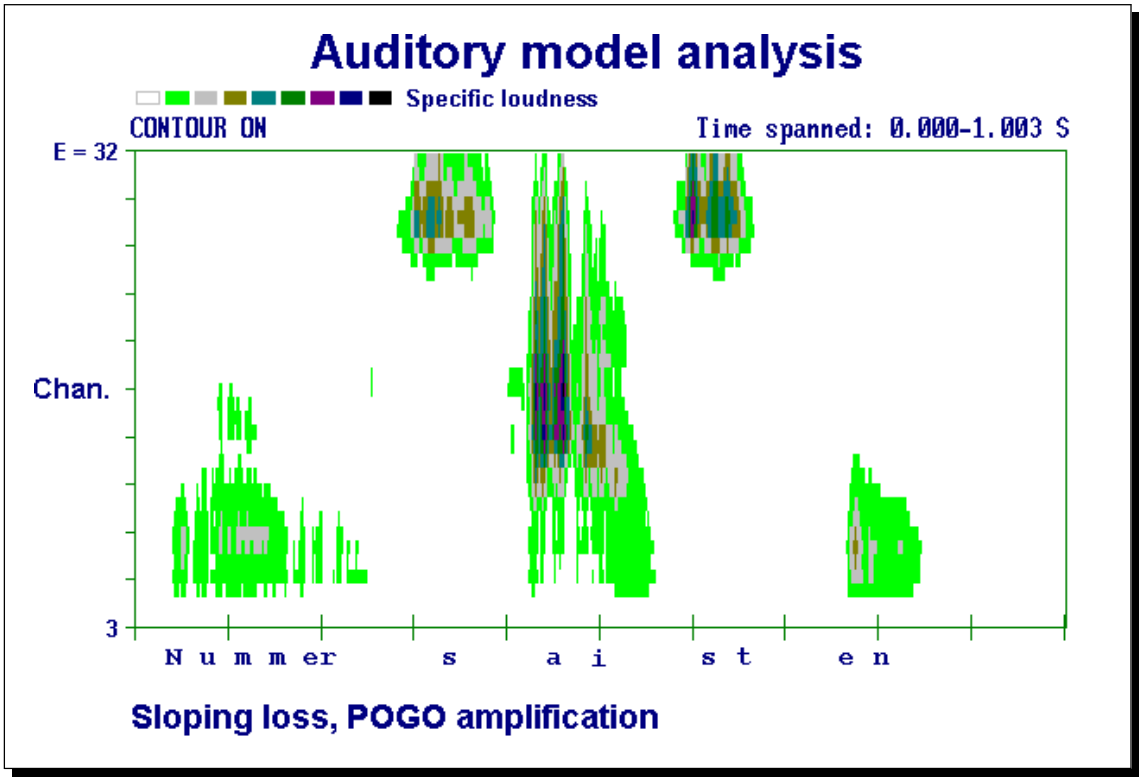

25. *The danish utterance "Nummer saisten" (Number sixteen) processed through the auditory model with a typical sensorineural, sloping hearing loss, and viewed as a grey-scale mapping of specific loudness. The signal level was set at 65 dB SPL, and amplification was applied according to the POGO rule. The x-axis is time and the y-axis is channel number in the model.*

The amplification ensures more loudness and audibility for loud sounds, but the weak sounds are not visible. Furthermore, the increased upward spread of masking causes the audible sounds to be spread across more channels as seen for the vowel 'a'.

5.2 Performance and future improvements.

The above examples show how the model is useful for a visualization of hearing-impaired perception of complex sounds, and thus for a qualitative analysis of hearing-aid processed signals. For a quantitative analysis, the current graphing program

(imported into HyperSignal Workstation) is not adequate, and future versions of the model should rather include dedicated graphing functions.

The model performs the processing of this 1-second signal in 111 seconds on a 486/25 MHz PC, using 256-point signal frames that were overlapped 75%. It is thus useful for immediate analysis of short signals. For longer signals, several signals could for instance be processed overnight in a batch-file.

6 Conclusion.

An auditory model based on psychoacoustic theory has been presented. The advantage of this approach, rather than using a physiological model, was discussed. The model has been specified, developed and implemented based on selected results from the literature. As an attempt to unify various psychoacoustic models for filter shapes, loudness growth etc., the model represents a compromise that can be subject to controversies.

The elements of the model are: Power spectrum calculation, equalizations and coupler corrections, an auditory filter bank with or without hearing loss, and loudness growth functions for normal and impaired hearing. The temporal properties of the normal and impaired hearing system have not been included in the current implementation, due to time limitations in the project.

The model was verified against various results from the psychoacoustic literature. For normal hearing, the model reproduced masking patterns for narrow-band noise well, underestimating upward spread of masking at high masker levels. For hearing-impaired subjects, the upward spread of masking was furthermore limited by the upper frequency limit used for the simulations. Nevertheless, the model correctly reproduced narrow-band masked thresholds well for a small, selected group of impaired subjects.

The loudness growth function was generally correct, but loudness was underestimated at high levels, compared to the usual 0.3 power law used at high levels. This discrepancy was also due to the frequency limit in the model. As a consequence, the equal loudness level contours for normal hearing were also incorrect at high levels. For impaired hearing, the model also produced the proper loudness growth according to Zwicker & Fastl (1990), but in disagreement with an alternative loudness model used by Hellman & Meiselman (1990).

Based on the above simulations and verifications of the model, it can be justified, that the model represents known psychoacoustic properties of the normal and impaired human ear, with the exception of temporal properties.

As an example of a real-world application of the model, loudness spectrograms for a speech utterance were presented. By introducing hearing loss, the speech sounds became less audible and less detailed, a problem that linear amplification did not solve properly. This demonstrated how the model could be used for hearing aid development and evaluation.

Future improvements of the model include: Models of temporal processing for normal hearing and hearing impairment. Also graphical output and a more user-friendly interface might be added.

7 References.

Agerkvist, F.A. (1992). Time-frequency analysis with temporal and spectral resolution as the human auditory system. Proc. IEEE-SP Int. Symp. on Time-Frequency and Time-Scale analysis. Vancouver, BC, Canada, 1992.

Allen, J.B. (1985). Cochlear modeling. IEEE ASSP Magazine, January 1985.

Allen, J.B. (1990). Modeling the noise damaged cochlea. In: The Mechanics and Biophysics of Hearing. (ed. Dallos, Geisler, Matthews, Ruggero & Steele), Springer, Berlin, 1990.

Allen, J.B, Hall, J.L. and Jeng, P.S. (1990). Loudness growth in 1/2 octave bands (LGOB) - A procedure for the assessment of loudness. J Acoust Soc Am, 88(2), 745 - 753.

Barfod, J. (1976). Multichannel compression hearing aids. Report no. 11, The Acoustics Laboratory, Technical University of Denmark.

Berger, E.H. (1981). Re-examination of the low-frequency (50 - 1000 Hz) normal thresholds of hearing in free and diffuse sound fields. J Acoust Soc Am, 70(6), 1635 - 1645.

Bentler, R.A. and Pavlovic, C.V. (1989). Transfer functions and Correction Factors Used in Hearing Aid Evaluation and Research. Ear Hear, 10(1), 58 - 63.

Bentler, R.A. and Pavlovic, C.V. (1992). Addendum to "Transfer functions and Correction Factors Used in Hearing Aid Evaluation and Research". Ear Hear, 13(4), 284 - 286.

Buus, S. (1992). Experiments with an auditory model and auditory filter spacing. Personal communication.

Buus, S. & Florentine, M.(1992). Recent results on free-field monaural thresholds. Personal communication.

Cohen, J (1989). Application of an auditory model to speech recognition. J Acoust Soc Am, 85(6), 2623 - 2629.

de Boer, E. (1985). Auditory Time Constants: A paradox? In: Time Resolution in Auditory Systems. (ed. Michelsen). Springer, Berlin, 1985

Dubno, J.R. & Schafer, A.B. (1992). Comparison of frequency selectivity and consonant recognition among hearing-impaired and masked normal-hearing listeners. J Acoust Soc Am, 91(4), 2110 - 2121.

Evans, E.F. (1975a). Cochlear nerve and cochlear nucleus. Chapter 1 in: Handbook of sensory physiology, vol. V/2: Auditory system. (ed: Keidel, W.D. and Neff, W.D). Springer-Verlag, New York, pp. 1 - 96.

Evans, E.F. (1975b). The sharpening of cochlear frequency selectivity in the normal and abnormal cochlea. Audiology 14, 419 - 442.

Evans, E.F. (1985). Aspects of the neural coding of time in the mammalian peripheral auditory system relevant to temporal resolution. in: A Michelsen (ed.). Time resolution in auditory systems. Springer, Berlin, pp. 74 -95.

Evans, E.F. and Elberling, C. (1982). Location-Specific Components of the Gross Cochlear Action Potential. Audiology 21, 204 - 227.

Fink, F. (1989). Introduktion til auditiv modellering (Danish). Publ. R 89-8, Institute of Electronics Systems, Aalborg University Center.

Florentine, M., Buus, S., Scharf, B. and Zwicker, E. (1980). Frequency selectivity in normally-hearing and hearing-impaired observers. J Speech Hear Res 23, 646 - 669.

Florentine, M. and Zwicker, E. (1979). A model of loudness summation applied to noise-induced hearing loss. Hear Res 1, 121 - 132.

Glasberg, B.R. and Moore, B.C.J. (1986). Auditory filter shapes in subjects with unilateral and bilateral cochlear impairments. J Acoust Soc Am, 79(4), 1020 - 1033.

Glasberg, B.R. and Moore, B.C.J. (1990). Derivation of auditory filter shapes from notched-noise data. Hear Res 47, 103 - 138.

Harrison, R.V. and Evans, E.F. (1982). Reverse correlation study of cochlear filtering in normal and pathological guinea pig ears. Hear Res 6, 303 - 314.

Hellman, R.P. and Meiselman, C.H. (1990). Loudness relations for individuals and groups in normal and impaired hearing. J Acoust Soc Am, 88(6), 2596 - 2606.

Hermansky, H. (1990). Perceptual linear predictive (PLP) analysis of speech. J Acoust Soc Am, 87(4), 1738 - 1752.

Hirahara, T. and Komakine, T. (1989). A computational cochlear nonlinear preprocessing model with adaptive Q circuits. Proc ICASSP 1989, 496 - 499.

Humes, L.E., Espinoza-Varas, B., and Watson, C.S. (1988). Modeling sensorineural hearing loss. I. Model and retrospective evaluation. J Acoust Soc Am, 83(1), 188 -202.

Humes, L.E. and Jesteadt, W. (1991). Models of the effects of threshold on loudness growth and summation. J Acoust Soc Am, 90(4), 1933 -1943.

IEC 303 (1970). IEC provisional reference coupler for the calibration of earphones used in audiometry. 1. edition.

IEC 318 (1970). An IEC artificial ear, of the wideband type, for the calibration of earphones used in audiometry. 1. edition.

IEC 711 (1981). Occluded-ear simulator for the measurement of earphones coupled to the ear by ear inserts. 1. edition.

ISO 226 (1987). Acoustics - Normal equal-loudness level contours.

ISO/TC43/WG1/N160 (1991). Second Working Draft for a revision of ISO 226 (October 1991).

ISO 389 (1991). Acoustics - Standard reference zero for the calibration of pure tone air conduction audiometers.

Karjalainen, M. (1985). A new auditory model for the evaluation of sound quality of audio systems. Proc ICASSP 1985, Tampa.

Karjalainen, M. (1987). Auditory models for speech processing. Proc. Int. Congr. Phon. Sciences. Tallinn.

Kates, J.M. (1991). A time-domain digital cochlear model. IEEE Trans Sig Proc, 39(12), 2573 - 2592.

Killion, M.C. (1978). Revised estimate of minimum audible pressure: Where is the "missing 6 dB"? J Acoust Soc Am, 63(5), 1501 - 1508.

Killion, M.C. (1984). New insert earphones for audiometry. Hearing Instruments, 35, 45 - 46.

Leijon, A. (1989). Optimization of hearing-aid gain and frequency response for cochlear hearing losses (Ph.D. thesis). Technical report no. 189. Chalmers University of Technology, Göteborg, Sweden.

Liberman, M.C. and Dodds, L.W. (1984). Single-neuron labeling and chronic cochlear pathology. III. Stereocilia damage and alterations of threshold tuning curves. Hear Res 16, 55 - 74.

Lippman, R.P., Braida, L.D. and Durlach, N.I. (1981). Study of amplitude compression and linear amplification for persons with sensorineural hearing loss. J Acoust Soc Am, 69(2), 524 - 534.

Ludvigsen, C. (1985). Relations among some psychoacoustic parameters in normal and cochlearly impaired listeners. J Acoust Soc Am, 78(4), 1271 - 1280.

Lutfi, R.A. and Patterson, R.D. (1984). On the growth of masking asymmetry with stimulus intensity. J Acoust Soc Am, 74(3), 739 - 745.

Lyon, R.F. (1982). A computational model of filtering, detection and compression in the cochlea. Proc. ICASSP 1982, 1282 - 1285.

Lyon, R.F. and Dyer, L. (1986). Experiments with a computational model of the cochlea. Proc. ICASSP 1986, 1975 - 1978.

Lyon, R.F. and Mead, C.A. (1988). An analog electronic cochlea. IEEE Trans ASSP, 36(7).

Mehrgardt, S. and Mellert, V. (1977). Transformation characteristics of the external ear. J Acoust Soc Am, 61(6), 1567 - 1576.

Moore, B.C.J. and Glasberg, B.R. (1983). Suggested formulae for calculating auditory-filter bandwidths and excitation patterns. J Acoust Soc Am, 74(3), 750 - 753.

Moore, B.C.J., Glasberg, B.R., Hess, R.F. and Birchall, J.P. (1985). Effects of flanking noise bands on the rate of growth of loudness of tones in normal and recruiting ears. J Acoust Soc Am, 77(4), 1505 - 1513.

Moore, B.C.J. and Glasberg, B.R. (1986). The role of frequency selectivity in the perception of loudness, pitch and time. In: Frequency Selectivity in Hearing - chapter 5 (ed: B.C.J. Moore), Academic Press, London.

Moore, B.C.J. and Glasberg, B.R. (1987). Formulae describing frequency selectivity as a function of frequency and level, and their use in calculating excitation patterns. Hear Res, 28, 209 - 225.

Moore, B.C.J. and Glasberg, B.R. (1989). Difference limens for phase in normal and hearing-impaired subjects. J Acoust Soc Am, 86(4), 1351 - 1365.

Moore, B.C.J., Glasberg, B.R., Donaldson, E., McPherson, T. and Plack, C.J. (1989). Detection of temporal gaps in sinusoids by normally hearing and hearing-impaired. J Acoust Soc Am, 85(3), 1266 - 1275.

Moore, B.C.J. and Peters, R.W. (1990). Auditory filter shapes at low frequencies. J Acoust Soc Am, 88(1), 132 - 1140.

Neely, S.T. and Kim, D.O. (1983). An active cochlear model showing sharp tuning and high sensitivity. Hear Res, 9, 123 - 130.

Nielsen, Lars B. (1992). Subjective evaluation of sound quality for normal-hearing and hearing-impaired listeners. Internal report no. 43-8-1, Oticon Research Unit,

Snekkersten, Denmark. Also published as: Technical Report no. 51, The Acoustics Laboratory, Technical University of Denmark, Lyngby, Denmark.

ODIN (1988). FIRFILT High Speed FIR Filtering Program, revision 1.0. Report from ODIN-project, Otwidan, Copenhagen.

Patterson, R.D., Nimmo-Smith, I., Weber, D.L. and Milroy, R. (1982). The deterioration of hearing with age, the audiogram and speech threshold. J Acoust Soc Am, 72(6), 1788 - 1803.

Pavlovic, C.V. (1987). Derivation of primary parameters and procedures for speech intelligibility predictions. J Acoust Soc Am, 82(2), 413 - 422.

Peters, R.W. and Moore, B.C.J. (1992). Auditory filter shapes at low frequencies in young and elderly hearing-impaired subjects. J Acoust Soc Am, 91(1), 256 - 266.

Pickles, J.O. (1982). An introduction to the physiology of hearing. Academic Press, London.

Robinson, & Dadson (1956). A re-determination of the equal-loudness relation for pure tones. Brit J Appl Phys, 7, 166 - 181.

Scharf, B. (1978a). Comparison of normal and impaired hearing I: Loudness, localization. In: Sensorineural hearing impairment and hearing aids (eds.: Ludvigsen & Barfod). Scand Audiol, suppl. 6.

Scharf, B. (1978b). Loudness. Chapter 6 in: Handbook of Perception. Vol. IV: Hearing. (eds.: Carterette & Friedman). Academic Press, New York.

Scharf, B. and Buus, S. (1986). Audition I: Stimulus, Physiology, Thresholds. In: Handbook of perception and human performance, vol. I: Sensory Processes and Perception (eds.: Boff, K.R., Kaufmann, L. & Thomas, J.P.) Wiley-Interscience, New York.

Scharf, B. and Houtsma, A.J.M. (1986). Audition II: Loudness, Pitch, Localization, Aural Distortion, Pathology. In: Handbook of perception and human performance, vol. I: Sensory Processes and Perception (eds.: Boff, K.R., Kaufmann, L. & Thomas, J.P.) Wiley-Interscience, New York.

Schwartz, D.M., Lyregaard, P.E. & Lundh, P. (1988). Hearing aid selection for Sever-to-Profound Hearing Loss. Hearing Journal, 39(2), 13 - 17.

Seneff, S. (1984). Pitch and spectral estimation of speech based on auditory synchrony model. Proc. ICASSP 1984.

Seneff, S. (1985). Pitch and spectral analysis of speech based on an auditory synchrony model. M.I.T. Technical Report 504, 242 pp.

Shailer, M.J., Moore, B.C.J., Glasberg, B.R., Watson, N. and Harris, S. (1990). Auditory filter shapes at 8 and 10 kHz. J Acoust Soc Am, 88(1), 141 - 148.

Shaw, E.A.G. (1974). Transformation of sound pressure level from the free field to the eardrum in the horizontal plane. J Acoust Soc Am, 56(6), 1848 - 1861.

Shaw, E.A.G. and Vaillancourt, M.M. (1985). Transformation of sound pressure level from the free field to the eardrum presented in numerical form. J Acoust Soc Am, 78(3), 1120 - 1123.

Stone, M. (1992). Recent data on auditory filter shapes for hearing-impaired listeners. Personal communication.

Tyler, R.S., Hall, J.W., Glasberg, B.R., Moore, B.C.J. and Patterson, R.D. (1984). Auditory filter asymmetry in the hearing-impaired. J Acoust Soc Am, 76(5), 1363 - 1368.

Tyler, R.S. (1986). Frequency resolution in hearing-impaired listeners. In: Moore, B.C.J. (ed.). Frequency selectivity in hearing. Academic Press.

Zwicker, E. & Fastl, H. (1990). Psychoacoustics - facts and models. Springer-Verlag, Berlin.

Zwicker, E. & Feldtkeller, R. (1967). Das Ohr als Nachrichtenempfanger. Hirzel, Stuttgart.

Zwicker, E. & Terhardt., E. (1979). Automatic speech recognition using psychoacoustic models. J Acoust Soc Am, 65(2), 487 - 498.

Zwislocki, J.J. (1965). Analysis of some auditory characteristics. In: Luce, RD, Bush, RR and Galanter, E (eds.). Handbook of Mathematical Psychology, Vol. III. Wiley, New York.

8 Appendices.

8.1 User manual.

The auditory model has been written in the C language and compiled and debugged using the Borland Turbo C++ 1.0 compiler. It runs on any IBM PC-AT compatible computer with a mathematical co-processor. For processing of long signals, at least a 386DX - 25 MHz is recommended due to the heavy computation load in the model. The entire model is contained in a single executable, AUDMOD.EXE, which is provided on a disk along with a few sample input parameter files. The flow of the program is illustrated in figure 26.

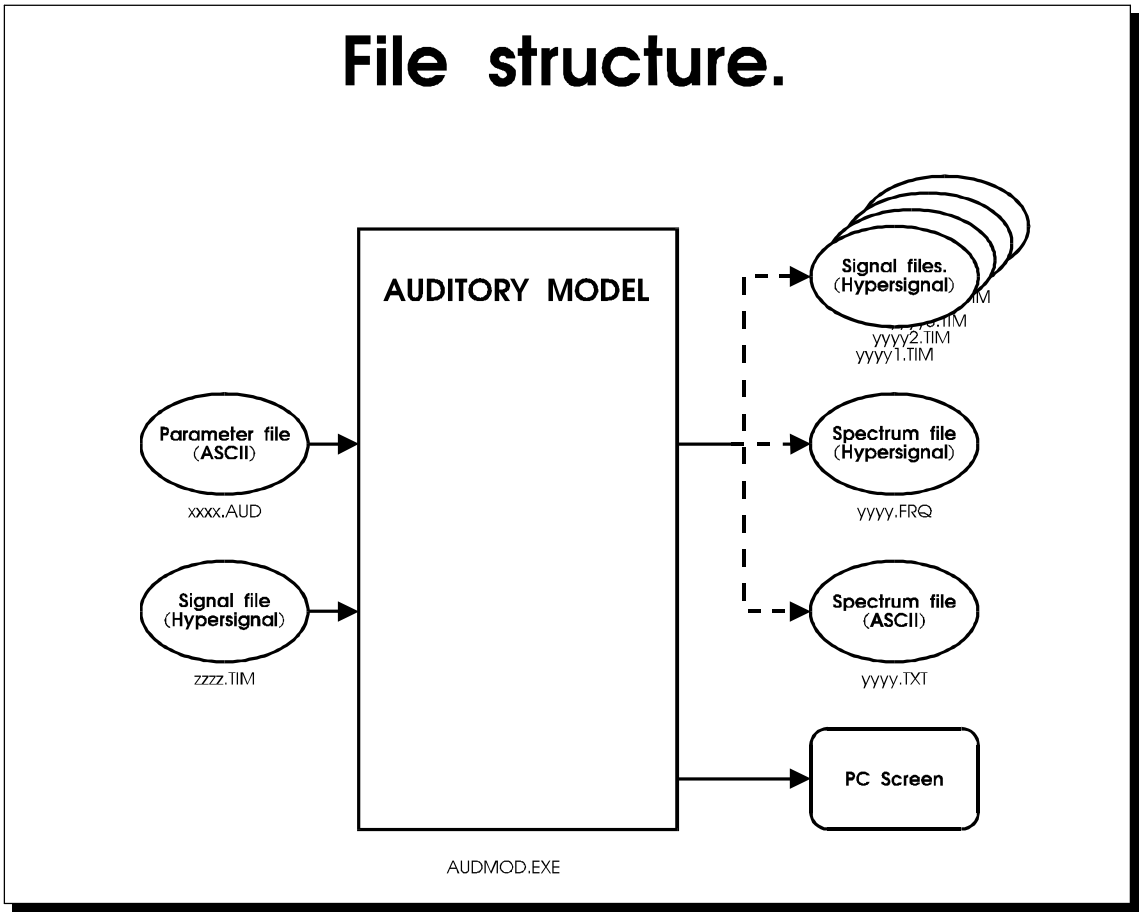

26. *Block-diagram indicating the file structures and data flow in the auditory model. Two input files are required: .AUD parameter file and .TIM signal file. The model output is sent to the screen (can be redirected to a file) and to an output file in either Hypersignal binary format (.FRQ) or in an ASCII text file (.TXT).*

8.1.1 Input parameter file format.

The .AUD input parameter file specifies all the free parameters in the model. These parameters must be in a particular order, as shown below. A line that begins with a non-white character (i.e. not a tab, space or new line character) is considered an input line, whereas a line beginning with a white character is ignore. All indented lines can thus be used for comments. A valid input line requires the accurate spelling of the parameter, followed by one or more tabs and/or spaces, and the value of the parameter. A sample parameter file is shown in figure 27.

```
        AUDITORY MODEL PARAMETERS

        Filename:              test41.aud
        Date:                  28.12.92
        Time:                  15:00
        Notes:                 30 channel FFT-based model, using roex filters.
                               Excitation patterns, white noise, 10 db steps

                               All indented lines are ignored.
                               Model parameters follow in order:

No. channels:                  30
Lower E limit:                 3
Upper E limit:                 32
Output channel:                0
                               0 for all channels.
Output level:                  0
                               0 for end of model.
Input sample rate (Hz):        20000
dB SPL of cal. sinus:          60
Peak value of cal. sin:        16358
                               sqr(2)*noise signal rms value
Recording coupler:             1
                               1: Free field, 2: IEC711/KEMAR, 3: IEC303
Transmission factor:           1
                               1: Zwicker's A0, 2: ELC 100, 3: ELC100 flat bl. 1 kHz
Binaural:                      0
                               0: Monaural, else binaural loudness
Output sample rate(Hz):        0
                               If 0, based on input sample rate, frame size and
overlap
Input frame size:              256
                               Must be power of two and no more than 8192
Overlap:                       0
                               No overlap
Process:                       8
                               0 = all frames, 1 = single frame, n = #frames to
average
Output frame size:             100
No. frames to process:         0
                               0 for all frames.
No. zero frames to add:        0
                               The input signal can be padded with zeros
                               if model has post-masking.
Output format:                 11
                               Can be 1 time series per file:
                               or output as vectors:
                               Hypersignal FRQ (10), int (11) or float (12)

Audiogram (Hz):   125   250   500   750   1000  1500  2000  3000  4000  6000  8000
Audiogram (dB HL):0     0     0     0     0     0     0     0     0     0     0
UCL (dB HL):      120   120   120   120   120   120   120   120   120   120   120
```

27. *Sample parameter file for auditory model. All indented lines are ignored by the model, serving as comments.*

Since all indented lines are ignored by AUDMOD.EXE, the first few lines in figure 27 are comments to aid the user. The input parameters then follow:

1. **No. channels:** Number of output channels in the auditory model. The spacing between the channels in E-units is determined by the upper and lower limits on the E-scale as defined in the following two parameters.

The number of channels has been 30 in the current report corresponding to roughly 7 kHz bandwidth in the model. In the case of an .FRQ output file, the number of channels is rounded up to nearest power of two plus one (i.e. 33 channels), and the E-spacing is consequently reduced.

2. **Lower E limit:** The center E-value for the lowest band in the model. E = 3 corresponds to 87 Hz.

3. **Upper E limit:** The center E-value for the highest band in the model. E = 32 corresponds to 6.97 kHz.

4. **Output channel:** Only relevant in the case of the output being specified as one waveform file per channel (**Output format:** 0). One particular channel can be selected here, if the other waveform files are irrelevant. Usually set to 0, meaning that all channels are output.

5. **Output level:** This specifies at which point in the model, the output frames are written to the output file as follows (see figure 1):

   5: ERB-power
   6: Excitation from *roex* filterbank (*E*).
   7: Specific loudness = end of model.
   0: End of model. (could change in the future).

6. **Input sample rate:** Sample rate for input file. Normally overridden by the sample rate specified in the input waveform (.TIM) file header. Can be checked on the output screen from the model.

7. **dB SPL of cal. sinus:** For absolute sound pressure level calibration of the model. Assume, for example, that we have recorded a calibration sine wave to a waveform file using the same electrical gain from the microphone to the A/D-converter as used for recording of the signals for analysis. The actual dB SPL value of the calibration signal (typically 94 dB SPL, for a B&K 4230 calibrator) read from the measurement amplifier should then be written down and entered here. The dB SPL parameter can also be used for 'artificial' signals or to scale signals up or down to force a given dB SPL-calibration.

8. **Peak value of cal. sinus:** From the above example, the peak value of the sine wave in the signal file must then be determined. This can be done in a signal-editor (such as HyperSignal Workstation) or by means of a peak-detecting program. If the signal is noisy, or not a sine wave, this peak value cannot be estimated easily. In this case, it is better to determine the long-term RMS-value and multiply it by $\sqrt{2}$. The small utility RMS.EXE (Nielsen, 1992) can be used to calculate RMS- and peak values for Hypersignal .TIM waveform files.

By means of parameters 7. and 8. a signal can be set to the desired SPL-value by determining the long-term RMS-value of the signal file, multiply by $\sqrt{2}$ to get parameter 8, and setting the dB SPL (parameter 7) to the desired value.

9. **Recording coupler:** If a signal was recorded by means of a microphone, the auditory model must know at which point the signal was recorded. There are three options available, which are set by numerical value:

   1: Recorded in free field (or reverberant), i.e. a microphone in a room.
   2: Recorded at the eardrum, in KEMAR, or in an IEC 711 ear simulator.
   3: Recorded in an IEC 303 (6 cm^3) coupler.

   Most real-world or synthetic signals should be referred to free-field (**1**), as they were recorded in a room, or assumed to be reproduced by a loudspeaker with a flat frequency response. If the signal is referred to the eardrum (e.g. the tympanic membrane, parameter value **2**), the auditory model must divide the input spectrum by the open-ear response. Similarly, a coupler frequency response correction is applied in the case of an IEC 303 coupler (value **3**). See section 3.3 for further discussion on coupler corrections.

10. **Transmission factor:** Specifies the fixed frequency response equalization applied to the input spectrum (after correcting for coupler response) before passing it through the auditory filterbank. The parameter choices are:

    1: Zwicker a_0 transmission factor.
    2: 100-phone equal-loudness contours.
    3: 100-phone equal-loudness contours, flat below 1 kHz.

    See section 3.3 for details.

11. **Binaural:** For selection of monaural or binaural listening. Monaural (**0**) is obviously used for eardrum recordings or with hearing aid. The binaural (**1**) condition applies to a symmetric binaural situation, ie. symmetric hearing loss listening in the vertical plane only (azimuth = 0).

12. **Output sample rate (Hz):** Specifies the sample rate, i.e. the time intervals between successive output frames. This is accomplished by forcing the overlap between input frames to the right value. By setting the output sample rate to **0**, it will instead be calculated based on sample rate, input framesize and overlap and forced to this value.

13. **Input frame size:** The width, in samples, of successive input frame. Due to the FFT used for calculation of the spectrum, the frame size must be a power of two from the following set of values: 128, 256, 512, 1024,

2048, 4096, 8192. For the simulations in this model, 256 point frames were used, corresponding to 12.8 ms frame width at 20 kHz sample rate.

14. **Overlap:** The overlap, in samples, between successive input frames. 0 means no overlap, i.e. the input frames are side-by-side. The highest value is input frame size - 1, corresponding to a 1 sample increment in the input signal after reading a new frame. For 75% overlap, which was used for the speech signals in section 5.1., the overlap value must be set to 192.

15. **Process:** Used to specify an optional spectral averaging. 0 means that all frames average into one long-term power spectrum. Useful for stationary noise signals. 1 means single frame, i.e. no averaging. Any other positive integer specifies the number of successive input frames to be averaged into 1 output frame. For instance, 8 means that 8 input frames at a time are averaged to form one output frame.

16. **Output frame size:** For time-domain output files, (Output format 0), this is the frame size of each output file. In the case of frequency-domain files (Output format 10 or 11), this specifies how many frames are stored internally, before being written to file. In the latter case, this number is not critical, and a typical value of 100 can easily be used without any memory problems.

17. **No. frames to process:** Number of input frames to process, before terminating program. 0 means the entire input file, any other number is used to specify a smaller number of frames, ie. not the entire file.

18. **No. zero frames to add:** Optional number of frames containing zeros, that are padded to the input signal file. Useful for a future version of the model that contains post-masking, so that the model is allowed to settle after the input signal has been turned off.

19. **Output format:** Three choices are available for output file formats:

    0: .TIM time-domain waveform files, with one channel per file. For N channels, N output files are created, using the first six letters of the output file name plus two digits to form the file name XXXXXXNN.TIM, where NN is the channel number of the output file. These files are in HyperSignal Workstation format, where they can be viewed and manipulated.

    10: .FRQ frequency domain files with consecutive frames stored in one file. Each output 'spectrum' is stored as a 16-bit integer value in a frame. The file can be viewed and manipulated further in HyperSignal Workstation. The speech processing examples in figures 23, 24 and 25 have been made from Hypersignal screen outputs.

11: .TXT text output files: This file contains header information, followed by channel information (E-value, center frequency), followed by the actual data, frame-by-frame. For each frame, separate lines are printed for the ERB-power, the filterbank output (excitation), and specific loudness. The output file can be imported into a spreadsheet, such as Microsoft Excel, with each line forming one row. The data values in the .TXT file are delimited by tab characters, which is converted into separate columns in Excel.

20. **Audiogram (Hz):** The audiogram frequencies, listed in order. In the current implementation, these are not optional, but must be (in order): 125, 250, 500, 750, 1000, 1500, 2000, 3000, 4000, 6000, 8000. In the case of missing intermediate frequencies, these can be interpolated on an audiogram form.

21. **Audiogram (dB HL):** The hearing loss at each of the audiogram frequencies listed above. Normal hearing corresponds to 0 dB HL for all frequencies.

22. **UCL (dB HL):** The uncomfortable levels at each of the audiogram frequencies, expressed in dB HL. This line must be included, but the proposed UCL encoding scheme (Appendix 8.2) has not been evaluated. The UCL effect can effectively be disabled by specifying large values, e.g. 120 dB HL across all frequencies.

8.1.2 Command-line usage.

Many of the input file parameters can be overridden on the DOS command-line. The command-line format is the following:

```
AUDMOD parmfile infile outfile [switches]
```

where

`parmfile` is the auditory model parameter file base name (see above for format). The file extension .AUD should not be included, since it is added by the program automatically.

`infile` is the input waveform file (.TIM - Hypersignal format). The file extension .TIM should not be included, since it is added by the program automatically.

`outfile` is the output file base name. In the case of time waveform output files (Output format 0), the base name is truncated to 6 letters, and the remaining two characters are used for channel numbering. The file extension .TIM is appended automatically. In the case of spectrum output files (.FRQ - format 10 or .TXT - format 11), there is only one output file, and the appropriate file extension is appended automatically.

The optional command-line switches are listed in Figure 28. In the cases where they duplicate parameter file values, the command-line values are used.

```
AUDMOD   :  Auditory model signal processing.
            Copr.(C)   Lars Bramsløw Nielsen
            Revision: 1.3       Date: Jan 15 1993

Usage    : AUDMOD parmfile infile outfile [switches]

 parmfile: ASCII file with model setup parameters (.AUD)
   infile: HS time series file containing input signal (.TIM)
  outfile: HS time series file name for output (max. 6 char)
           2 digits appended for channel number
 Optional processing switches override parmfile setttings:
      /c#: Channel signal to be output, default all channels.
      /l#: Output level in model, 1 = first stage etc.. , 0 = all.
      /o#: Output format, 0 = .TIM, 10 = .FRQ.
      /f#: Number of frames to process, default all.
      /s#: Framesize, 128 - 8192 (power of two).
      /t#: Number of milliseconds to process, default all.
      /p#: Spectrum processing: 0 = single frame,
           1 = power spectrum averaging.
      /b#: Binaural/Monaural loudness: 0 = Mon., 1 = Bin.
      /d : Debug mode - print more info.
```

28. *AUDMOD help screen specifying the required file names and the optional command-line parameters.*

Assuming that all values in the parameter file are specified correctly, the model can be run on a given input signal. There are self-explanatory error-messages in the case of illegal input file format or incorrect or conflicting input parameter values. A typical session then produces the screen output shown in Figure 29:

```
C:\DSP\AUDMOD\EVAL>audmod test41 uen_2db jtest > audmod.out


AUDMOD   :  Auditory model signal processing.
            Copr.(C)   Lars Bramsløw Nielsen.
            Revision: 1.3       Date: Dec 28 1992

------------------------- Processing Parameters -------------------------

Parameter file: test41.AUD                Recording coupler: Free field
Signal file: uen_2db.TIM                  Transmission factor: a0 (Zwicker)
Output file(s): test                      Monaural loudness.

Input sample rate: 20000.0 Hz             Input frame size: 256
Overlap: 0                                Number of input frames: 208
Spectrum averaging: 8 frames.
Number of channels:  30                   Output channel: All
E-start, E-end: 3.0, 32.0                 E-step: 1.000
Output sample rate:   78.1 Hz
Output level: End of model.               Output format: 11

Hit 'Esc' to terminate processing.

Frame #    8.         Power:     1.58       dB SPL     Loudness:  0.000      son
Frame #    16.        Power:     3.50       dB SPL     Loudness:  0.000      son
Frame #    24.        Power:     1.58       dB SPL     Loudness:  0.000      son
Frame #    32.        Power:     3.50       dB SPL     Loudness:  0.000      son
Frame #    40.        Power:     5.67       dB SPL     Loudness:  0.000      son
Frame #    48.        Power:     7.20       dB SPL     Loudness:  0.000      son
Frame #    56.        Power:     9.40       dB SPL     Loudness:  0.000      son
Frame #    64.        Power:     11.33      dB SPL     Loudness:  0.000      son
Frame #    72.        Power:     13.01      dB SPL     Loudness:  0.000      son
Frame #    80.        Power:     15.43      dB SPL     Loudness:  0.000      son
Frame #    88.        Power:     17.34      dB SPL     Loudness:  0.000      son
Frame #    96.        Power:     18.98      dB SPL     Loudness:  0.000      son
Frame #    104.       Power:     21.30      dB SPL     Loudness:  0.003      son
Frame #    112.       Power:     23.63      dB SPL     Loudness:  0.041      son
Frame #    120.       Power:     25.85      dB SPL     Loudness:  0.112      son
Frame #    128.       Power:     27.66      dB SPL     Loudness:  0.175      son
Frame #    136.       Power:     29.95      dB SPL     Loudness:  0.312      son
Frame #    144.       Power:     31.36      dB SPL     Loudness:  0.418      son
Frame #    152.       Power:     34.00      dB SPL     Loudness:  0.641      son
Frame #    160.       Power:     35.39      dB SPL     Loudness:  0.819      son
Frame #    168.       Power:     36.79      dB SPL     Loudness:  0.998      son
Frame #    176.       Power:     39.36      dB SPL     Loudness:  1.363      son
Frame #    184.       Power:     41.59      dB SPL     Loudness:  1.715      son
Frame #    192.       Power:     43.33      dB SPL     Loudness:  2.055      son
Frame #    200.       Power:     45.22      dB SPL     Loudness:  2.498      son
Frame #    208.       Power:     47.10      dB SPL     Loudness:  2.942      son
Frame #    216        Power:     50.16      dB SPL     Loudness:  3.782      son
Frame #    224        Power:     51.22      dB SPL     Loudness:  4.153      son
Processing completed.
```

29. *Typical screen output from the auditory model. The output can be directed to a file, and columns are separated by Tab's to facilitate import into a spreadsheet.*

The screen output can be redirected to a file in the usual DOS manner:

```
AUDMOD parmfile infile outfile [switches] > scrnfile
```

In this file, the columns are separated by tab characters, for easy import into a spreadsheet. The redirection does not apply to error messages, thus these are always forced to the screen (stderr, in UNIX and C terms).

8.2 Proposed UCL-encoding.

This encoding has been implemented in the model but has not been evaluated. The data from Allen et al (1990) show a steeper section on the average loudness growth curve for normal hearing subjects above the LOUD rating (= 6, equivalent to app. 50 sones). A similar pattern appears for individual hearing-impaired listeners. The standard loudness curve is thus modified by adding a steep, almost vertical, section to the specific loudness curve near UCL:

$$N_{UCL}^{\hat{A}} = \frac{N^{\hat{A}}}{\left[1-\left(\frac{E}{E_{UCL}}\right)^{\frac{1}{0.23}}\right]} \qquad \textbf{(23)}$$

The modification, implemented in the denominator approaches zero rapidly when E approaches E_{UCL}. The exponent 1/0.23 has been chosen somewhat arbitrarily to obtain a sharp transition close to UCL.

The values of E_{UCL} are found in the same fashion as for E_{TQ}, by presenting a shaped spectrum equivalent to the pure-tone UCLs. As for threshold values, discrepancies between the simultaneously presented UCL-shaped spectrum and the UCL measurement procedure with one tone presented at a time may be of importance here. The UCL feature has been implemented, but not tested against experimental data.